Knowledge and Information Systems (2020) 62:1279–1312
https://doi.org/10.1007/s10115-019-01382-x

REGULAR PAPER

Trajectory splicing

Qiang Lu[1] · Rencai Wang[1,3] · Bin Yang[2] · Zhiguang Wang[1]

Received: 23 September 2018 / Revised: 25 June 2019 / Accepted: 30 June 2019 / Published online: 18 July 2019

Abstract
With continued development of location-based systems, large amounts of trajectories become available which record moving objects' locations across time. If the trajectories collected by different location-based systems come from the same moving object, they are *spliceable trajectories*, which contribute to representing holistic behaviors of the moving object. In this paper, we consider how to efficiently identify spliceable trajectories. More specifically, we first formalize a spliced model to capture spliceable trajectories where their times are disjoint, and the distances between them are close. Next, to efficiently implement the model, we design three components: a disjoint time index, a directed acyclic graph of sub-trajectory location connections, and two splice algorithms. The disjoint time index saves a disjoint time set of each trajectory for querying disjoint time trajectories efficiently. The directed acyclic graph contributes to discovering groups of spliceable trajectories. Based on the identified groups, the splice algorithm *findmaxCTR* finds maximal groups containing all spliceable trajectories. Although the splice algorithm is efficient in some practical applications, its running time is exponential. Therefore, an approximate algorithm *findApproxMaxCTR* is proposed to find trajectories which can be spliced with each other with a certain probability within polynomial run time. Finally, experiments on two datasets demonstrate that the model and its components are effective and efficient.

Keywords Trajectory computation · Trajectory fusion · Trajectory recovery · Trajectory linking

✉ Qiang Lu
luqiang@cup.edu.cn

Rencai Wang
rcwang3@iflytek.com

Bin Yang
byang@cs.aau.dk

Zhiguang Wang
cwangzg@cup.edu.cn

[1] Beijing Key Lab of Petroleum Data Mining, China University of Petroleum-Beijing, Beijing, China

[2] Department of Computer Science, Aalborg University, Aalborg, Denmark

[3] IFLYTEK CO.,LTD, Hefei, China

1 Introduction

Information technology is almost everywhere in our daily life, which collects various information from different digital devices [4,10]. Specially, the location-based systems based on mobile devices, such as GPS, mobile phones, and near-field communication (NFC) terminals, generate large amounts of trajectories of moving objects. Usually, each individual system uses its unique *ID* code to identify each trajectory. For example, a mobile phone network identifies a trajectory by its telephone number, while an NFC system identifies it by its device-id. Since multiple systems may capture a same moving object at different times and places, each system gathers the object's partial trajectories. Recovering a **complete trajectory** of a moving object from these partial trajectories collected in various systems, named **trajectory splicing**, is essential for many applications, such as anomaly behavior detection [21,22], data fusion, and trajectory data mining [46]. The following case shown in Fig. 1 elaborates trajectory splicing.

Every weekday, Alice and Bob go to work by walking and taking the subway, as shown in Fig. 1. Their movements generate six partial trajectories: W1, S1, O1, W2, S2, and O2, where the mobile sport software captures W1 and W2; the subway check-in system captures S1 and S2; the office check-in system captures O1 and O2. Their complete trajectories can be recovered based on spatiotemporal locations of these partial trajectories. For example, S2 is more likely to splice with W2 than W1, because endpoint spatial positions of S2 are closer to those of W2, and the time interval of S2 [8:23,9:14] can be embedded into the time gap of W2 (8:20, 9:16). Similarly, O2 can splice with W2. So, connecting W2, S2, and O2 can repair Bob's whole trajectory.

According to the above case, finding a group of spliceable trajectories must satisfy the following three requirements. The first is the **disjoint time constraint** that requires that time intervals of spliceable trajectories in the group should not overlap with each other. The second is the **spatial constraint** that requires that the distances between their endpoints should be nearby with each other. The third is the **maximal group constraint** that requires that the group of spliceable trajectories should be maximal and should not be contained by other groups. That means connecting as many spliceable trajectories as possible to recover a complete trajectory.

However, it is non-trivial to find spliceable trajectories to satisfy the above constraints owing to the following three challenges. The first challenge is that the process of finding trajectories that satisfy the disjoint time constraint is very time-consuming. The process includes two steps: querying sub-trajectories in all time gap of a trajectory and counting the number of sub-trajectories that belong to the same trajectory. For example, in Fig. 1, W2 has three time gaps: $(-\infty$,8:00), (8:20,9:16), and (9:21,$+\infty)$. Querying sub-trajectories whose time intervals are in the three time gaps can obtain the sub-trajectory set $\{AB, EF, FS, S, C\}$. Then, the count based on the second step can get the set {S1(1), S2(1), W1(1), O1(1), O2(1)}, where W1(1) means W1 has one sub-trajectory in these time gaps. Since W1 has two sub-trajectories *DE* and *FS*, the time interval of W1 must overlap with that of W2. Therefore, the disjoint time set of W2 is {S1, S2, O1, O2}. If all trajectories have total M time gaps in the database, it needs to execute M^2 queries for finding disjoint time sets of all trajectories (Sect. 4). Although the index based on B^+-tree [7] or the data model of symbolic trajectories [13,17,29,35,40] can speed up each query, the time of total queries is still very long because M^2 is usually a vast number.

The second challenge is that the discovery of a group of spliceable trajectories is difficult. Relations between spliceable trajectories contain two categories. One is the **direct splice**

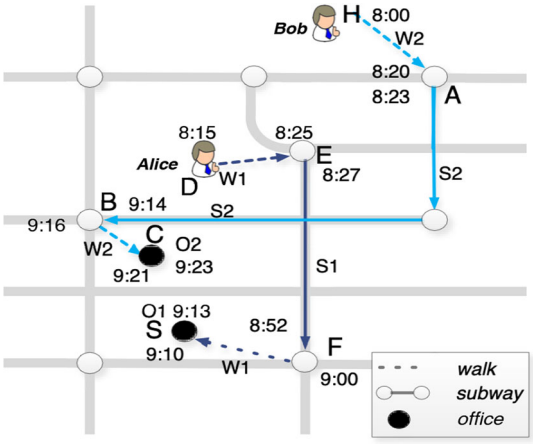

Fig. 1 The case of trajectory splicing

which connects two trajectories without using other spliceable trajectories. The other is the **indirect splice** which connects two trajectories by using other spliceable trajectories. For example, in Fig. 1, W2 and S2 are connected directly, while W2 and O2 are connected by S2. The indirect splice makes the process of splicing trajectories complicated because it needs to find other trajectories to determine whether the two trajectories can be connected or not. To the best of our knowledge, known group pattern mining [8,9,19,24–27,36,45] or trajectory clustering [24,25] cannot find groups of spliceable trajectories, because they discover groups of trajectories according to the similarity between them rather than the relation of direct (indirect) splice. Although fuzzy trajectory linking [38] is close to the challenge, it can only find two direct splice trajectories and is not suitable for mining multiple trajectories that are the direct or indirect splice.

The third challenge is that it must find as many spliceable trajectories of a moving object as possible. In general, if a method wants to acquire a group of spliceable trajectories which are not contained by other groups, it needs to traverse all possible combinations of spliceable trajectories for a moving object. For example, in the above case, to recover Bob's trajectory, these groups, such as {W2, S2}, {W2, O2}, {S2, O2}, and {W2, S2, O2}, must be traversed. Namely, it needs to find a group of spliceable trajectories which most compactly fill up a specific spatiotemporal range. So, it is a bin-packing problem and is NP-hard [23].The design of an approximation scheme or heuristic method is the key to deal with the problem.

In order to deal with the above challenges, a spliced model is defined to formalize the above requirements of spliceable trajectories. Based on the spliced model, trajectories are segmented into sub-trajectories according to a speed threshold. A B^+-tree [7] is used to save these sub-trajectories. For speeding up the process of finding disjoint time sets, the index of disjoint time called **DT-index** is constructed to keep intermediate results of searching the disjoint time set in each time slice. Moreover, the DT-index is a multi-resolution structure like a quadtree and can save intermediate results of time slices with different lengths, supporting queries with different time intervals. For example, assuming that the DT-index consists of intermediate results of one, two, and four days, if a query time interval is 4.5 days, the DT-index can find disjoint time sets within the four days, and the B^+-tree can find disjoint time sets within the 0.5 days. Based on the above two indexes, an algorithm ***queryDTsTR*** is proposed to obtain all disjoint time sets within a specific time interval.

In order to find spliceable trajectories, a directed acyclic graph of sub-trajectory location connections called ***STLC-DAG*** is created to connect sub-trajectories by their times and locations. Once the algorithm ***createSTLC-DAG*** has created the graph, it can obtain the spliceable sets of trajectories that can splice with a specific trajectory. For example, in the above case, the algorithm can find S2's spliceable set {W2}, W2's {S2, O2}, and O2's {W2}. Moreover, these spliceable sets form a **splice graph**, where each node is a trajectory, and the edge between two nodes represents that the two trajectories are spliceable. For instance, the node S2 has one edge which connects the node W2, and W2 has edges which connect S2 and O2. Thus, in the splice graph, a clique is a group of spliceable trajectories. For addressing the third challenge, an algorithm ***findMaxCTR*** is proposed to find all maximal groups of spliceable trajectories by listing all maximal cliques [34] in the graph. Although its worst running time is $O(3^{N/3})$, it can run very fast in many practical applications because the splice graph is usually very sparse [6]. Based on *findMaxCTR* and the splice graph, an approximate algorithm ***findApproxMaxCTR*** is proposed to find all maximal groups of approximate spliceable trajectories. Moreover, its running time is $O(N^2)$.

The main contributions in the paper are summarized as follows:

- A spliced model is introduced that can capture as many spliceable trajectories of a moving object as possible so that it can recover the complete trajectory of the moving object.
- The DT-index is designed to speed up the identification of the disjoint time set of each trajectory in a specific time interval.
- An algorithm *findMaxCTR* and its approximated algorithm *findApproxMaxCTR* are proposed to find maximal groups of spliceable trajectories or approximate spliceable trajectories, respectively.
- An empirical study conducted on real-world trajectories demonstrates that the proposed spliced model and algorithms are able to efficiently splice trajectories.

The remainder of the paper is organized as follows. In Sect. 2, we define the necessary concepts and formalize the spliced model. Then, we propose the two algorithms which discover groups of spliceable trajectories that satisfy the above definition in Sect. 3. Section 4 represents the theoretical analysis of these algorithms. Section 5 reports experimental results. We review the related work in Sect. 6 and conclude the paper in Sect. 7.

2 Problem definition

We introduce the necessary concepts and formalize the problem in the following section. Frequently used notation is listed in Table 1.

2.1 Basic concepts

A **sample point** $\boldsymbol{p = \langle id, lc, t \rangle}$ indicates that a moving object with identifier id is in location lc at timestamp t. A sample point may be a GPS, a photograph taken by a camera that is deployed at a road intersection or a check-in record. A **trajectory** (denoted as ***TR***) is a time-ordered sequence of sample points with a unique identifier. For example, in Fig. 2, $TR_A = \langle a_1, a_2, \ldots, a_9 \rangle$ is a trajectory of a moving object with identifier A.

However, a trajectory may not represent a continuous movement of a moving object because the moving object cannot be tracked at some time by a specific technology, such as W2 in Fig. 1. To represent the continuous movement of the moving object, we introduce the concept of **complete trajectory** (denoted as ***CTR***), which is a time-ordered sequence

Table 1 Notation

Notation	Definition
Ω	A *TR* database
p	A sample point $\langle id, lc, t \rangle$
TR_i	The ith *TR* in Ω
DT_i	A TR_i's disjoint time set
SP_i	A set of *TR*s that can be spliced with TR_i
STR_i^j	The jth sub-trajectory of ith *TR*
T	The time interval of query
N	The number of *TR*s in T
M	The number of all *STR* in T
CTR	A complete trajectory consists of spliceable *TR*s
$fst(S)$	Return the first element in sequence S
$lst(S)$	Return the last element in sequence S
$d(p, q)$	The Euclidean distance between two sample points p and q
$d(STR_i^j, STR_m^n)$	The Euclidean distance between two *STR*s
$ti(STR)$	The time interval of a sub-trajectory *STR*
$ti(TR_i)$	The time interval set of trajectory TR_i
$gap(STR_i^j, STR_m^n)$	The gap between two sub-trajectories
$gap(TR_i)$	The gap set of $ti(TR_i)$

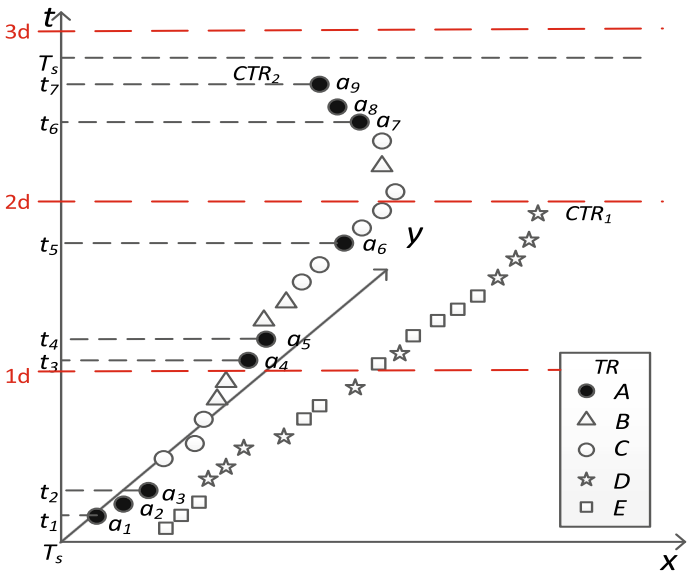

Fig. 2 Trajectory splicing

of all sample points that represent the same moving object but with different identifiers in different tracking systems. Thus, a complete trajectory may contain multiple trajectories that represent the same move object. For example, Fig. 2 shows the complete trajectories of two

moving objects: $CTR_1 = \{TR_A, TR_B, TR_C\}$, which includes the trajectories with identifiers A, B, and C, and $CTR_2 = \{TR_D, TR_E\}$, which includes the trajectories with identifiers D and E.

In a trajectory, two sample points, p_i and p_{i+1}, are **connectable** if $speed(p_i, p_{i+1}) \geq e$, where e is a speed threshold and

$$speed(p_i, p_{i+1}) = \frac{d(p_i, p_{i+1})}{|p_{i+1}.t - p_i.t|} \tag{1}$$

where $d(p_i, p_{i+1})$ returns the Euclidean distance between sample points p_i and p_{i+1}. Given a sequence of sample points in a trajectory TR_i, if any two consecutive sample points in the sequence are connectable, the sequence is **connectable** in that it shows one continuous movement. Moreover, if other connectable sequences do not contain a connectable sequence, the connectable sequence is called **sub-trajectory** (denoted as ***STR***). In particular, we use STR_i^j to denote the jth sub-trajectory in trajectory TR_i. For example, trajectory TR_A in Fig. 2 has 4 sub-trajectories: $STR_A^1 = \langle a_1, a_2, a_3\rangle$, $STR_A^2 = \langle a_4, a_5\rangle$, $STR_A^3 = \langle a_6\rangle$, and $STR_A^4 = \langle a_7, a_8, a_9\rangle$. A sub-trajectory is the **atomic** computational unit in this paper.

The **time interval** of the sub-trajectory, denoted as $\boldsymbol{ti}(STR)$, is $[first(STR).t, last(STR).t]$, where the function $first(\cdot)$ and $last(\cdot)$ return the first and last sample points in the sub-trajectory STR, respectively. The **time interval** of the trajectory is the set of time intervals of all its sub-trajectories, denoted as $\boldsymbol{ti}(\boldsymbol{TR_i}) = \bigcup_{STR_i^j \in TR_i} ti(STR_i^j)$.

The **gap** between two sub-trajectories STR_i^j and STR_m^n, denoted as $gap(STR_i^j, STR_m^n)$, is defined by Eq. 2.

$$gap(STR_i^j, STR_m^n) = (last(STR_i^j).t, first(STR_m^n).t) \tag{2}$$

Moreover, the **gap** of trajectory TR_i in the time interval T, denoted as $\boldsymbol{gap}(\boldsymbol{TR_i})$, is defined by Eq. 3.

$$gap(TR_i) = T - ti(TR_i) = T - \bigcup_{STR_i^j \in TR_i} ti(STR_i^j) \tag{3}$$

For example, the time interval of trajectory TR_A, denoted as $ti(TR_A)$, is $\{[t_1, t_2], [t_3, t_4], [t_5, t_5], [t_6, t_7]\}$. Given $T = [t_0, t_8]$, we have $gap(TR_A) = \{(t_0, t_1), (t_2, t_3), (t_4, t_5), (t_5, t_6), (t_7, t_8)\}$.

2.2 Spliceable trajectories

If two trajectories TR_i and TR_j can be spliced into a complete trajectory, they must meet the **disjoint time constraint** that requires that their interval times should not overlap each other, namely $ti(TR_i) \subset gap(TR_j)$. Given a trajectory TR_i, all the trajectories that meet the disjoint time constraint with TR_i constitute the **disjoint time set** of TR_i, denoted as DT_i. In Fig. 2, since $ti(TR_B) \subset gap(TR_A)$ and $ti(TR_C) \subset gap(TR_A)$, we have $DT_A = \{TR_B, TR_C\}$.

In addition to the aforementioned temporal constraint, if TR_i and TR_j are spliceable, they must also meet the **spatial constraint**, meaning that the sub-trajectories from TR_i and TR_j must be close enough to each other. To formally define the spatial constraint, we introduce two concepts—***spliceable pair*** and ***spliceable trajectories***.

Definition 1 Given two sub-trajectories STR_i^j and STR_m^n from two trajectories, respectively, and a distance threshold γ, if they do not overlap each other on the time dimension and

the distance between them is less than γ[1], the two sub-trajectories STR_i^j and STR_m^n form a ***spliceable pair*** , denoted as $\langle STR_i^j, STR_m^n \rangle$.

Definition 2 Given some trajectories, if the sub-trajectories in the given trajectories can constitute a sub-trajectory sequence $\langle STR_i^j, \ldots, STR_m^n \rangle$ such that any two neighbor sub-trajectories are a spliceable pair, these trajectories are called ***spliceable trajectories***.

Based on the above two definitions, we first introduce the concept—***complete trajectory*** to formulate the maximal group constraint, which requires that the group of spliceable trajectories should not be contained by other groups. Then, we define the ***splice degree*** to quantify the complete trajectory.

Definition 3 If other groups of spliceable trajectories do not contain a group of spliceable trajectories, the group forms a **complete trajectory**, denoted as ***CTR***.

Definition 4 The ***splice degree***, which consists of two factors: the ratio of the sum of the distances between different trajectories to the distance of *CTR* and the ratio of the sum of time gaps to the time interval of *CTR*, is used to quantify the compactness level of connections between trajectories in a *CTR*, defined by Eq. 4.

$$dg(CTR) = \frac{\sum_{\langle STR_i^j, STR_m^n \rangle \in CTR} d(STR_i^j, STR_m^n)}{distance(CTR)} \times \frac{\sum_{\langle STR_i^j, STR_m^n \rangle \in CTR} gap(STR_i^j, STR_m^n)}{time(CTR)} \tag{4}$$

where $\langle STR_i^j, STR_m^n \rangle$ is a *spliceable pair* in the *CTR*; $d(STR_i^j, STR_m^n)$ is the distance between two sub-trajectories STR_i^j and STR_m^n; $distance(CTR)$ is the sum of distances between two consecutive sample points in *CTR*, namely $distance(CTR) = \sum_{p_i \in CTR} d(p_i, p_{i+1})$, in which p_i and p_{i+1} are two consecutive sample points in the *CTR*; $time(CTR) = last(CTR).t - first(CTR).t$.

Based on the definition, $dg(CTR) \in (0, 1)$ and the smaller the splice degree $dg(CTR)$, the closer trajectories in the complete trajectory *CTR*. For example, in Fig. 2, assuming that the distance factors in Alice and Bob are the same value 0.02, $dg(\text{Alice}) = 0.02 \times (((8:27-8:25) + (9:00-8:52) + (9:13-9:10))/(9:13-8:15)) \approx 0.0448$, and $dg(\text{Bob}) = 0.02 \times ((8:23-8:20) + (9:16-9:14) + (9:23-9:21)/(9:23-8:00)) \approx 0.0017$. So, due to $dg(\text{Bob}) < dg(\text{Alice})$, the complete trajectory of Bob is better than that of Alice.

2.3 Problem definition

According to the above definitions, we formulate the problem of trajectory splicing by the trajectory splicing query.

Definition 5 From a dataset of trajectories, according to a query time interval, the ***trajectory splicing query*** discovers a complete trajectory sequence $CTRS = \langle CTR_1, \ldots, CTR_n \rangle$, where each complete trajectory *CTR* is ranked by its *splice degree*.

[1] Namely $(ti(STR_m^n) \subset gap(STR_i^j, STR_i^{j+1})) \cap (ti(STR_i^j) \subset gap(STR_m^{n-1}, STR_m^n)) \cap (d(last(STR_i^j), first(STR_m^n)) \leq \gamma)$.

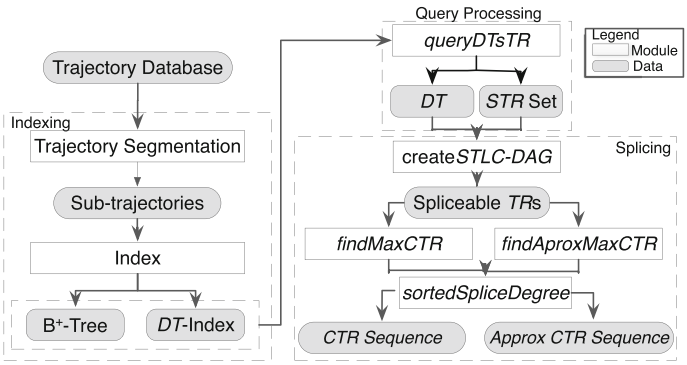

Fig. 3 The overview of trajectory splicing query

Based on the trajectories shown in Fig. 2, the trajectory splicing query finds a complete trajectory sequence $\langle CTR_1, CTR_2 \rangle$, where $CTR_1 = \{TR_D, TR_E\}$ and $CTR_2 = \{TR_A, TR_B, TR_C\}$.

3 The trajectory splicing query

We design a framework to execute the trajectory splicing query, which consists of three main modules: *indexing*, *query processing*, and *splicing*, as shown in Fig. 3.

In the indexing module, we first utilize the speed threshold e between two sample points to split trajectories into sub-trajectories (*STR*s). Then, we use a B^+*-tree* to index these sub-trajectories by their time intervals and create a disjoint time index (DT-index) to record the disjoint time set (DT) of each trajectory.

In the query processing module, based on the B^+*-tree* and the DT-index, we devise an algorithm *queryDTsTR* to search all sub-trajectories (*STR*s) and disjoint time sets (*DT*s) in a given time interval T.

In the splicing module, we first find spliceable trajectories by constructing the directed acyclic graph of sub-trajectory location connections (denoted as *STLC-DAG*). Next, we design an algorithm *findMaxCTR* to find a complete trajectory set, and an approximate algorithm *findApproxMaxCTR* to obtain the approximate complete trajectory set where each complete trajectory (*CTR*) represents a set of trajectories that can be spliced as much as possible. Finally, the two sets are ordered by the function of splice degree (Eq. 4) and form two sequences: a *CTR* sequence and an approximate *CTR* sequence, respectively.

3.1 Indexing sub-trajectories and the disjoint time set

3.1.1 B^+*-Tree*

To index a sub-trajectory *STR*, we first map it into a two-dimensional point in a coordinate system by applying the interval-spatial transform [7] to its time interval $ti(STR)$. For example, STR_A^1 in Fig. 2 is mapped into a point (t_1, t_2) according to $ti(STR_A^1)$.

Then, we insert the node *STR* into a B^+*-tree* by comparing its two-dimensional point with points of other nodes in the tree according the following rule [7]. Given two distinct points $\mathscr{P}_1 = (x_1, y_1)$ and $\mathscr{P}_2 = (x_2, y_2)$, $\mathscr{P}_1 < \mathscr{P}_2$ iff (a) $y_1 < y_2$; or (b) $y_1 = y_2$ and $x_1 < x_2$.

3.1.2 The disjoint time index

(1) ***Computing disjoint time set***

To support finding the **disjoint time set** DT_i of each trajectory TR_i in the different time intervals, we first partition the time dimension into time slices that have the same length d, e.g., an hour or a day. Then, precompute DT_i in every time slice, denoted as $DT_i^{k,d}$, where the superscripts k and d represent the time interval $[(k-1) \times d, k \times d]$. For example, as shown in Fig. 2, in the first time slice [0,d], $DT_A^{0,d} = \{B, C, D\}$ by searching trajectories that meet the disjoint time constraint (Sect. 2.2) in the above B^+*-tree*.

However, assuming the query time interval T that contains n time slices, we cannot ensure to obtain the **correct** disjoint time set DT_i in T only with the intersection of $DT_i^{k,d}$s on these n time slices. This is because sample points in a trajectory TR_j may not appear in a time slice so that $DT_i^{k,d}$ on the time slice does not contain the trajectory TR_j. For example, in Fig. 2, since the trajectory TR_E does not appear in $[2d, 3d]$, $DT_D^{3,d} = \phi$ and $DT_D = DT_D^{1,d} \cap DT_D^{2,d} \cap DT_D^{3,d} = \phi$. But, obviously $DT_D = \{E\}$ in $[0, 3d]$.

In order to overcome the above fault, the precomputation DF_i of each trajectory TR_i in any time slice needs to be executed by Eq. 5.

$$DF_i^{n+1,d} = \neg DT_i^{n+1,d} - \neg DT_i^{n,d} \tag{5}$$

where $\neg DT_i^{k,d} = P_i^{k,d} - DT_i^{k,d}$; $P_i^{k,d}$ is a set which contains all trajectories that appear in the kth time slice except the trajectory TR_i. For example, in Fig. 2, $P_A^{1,d} = P_A^{2,d} = \{B, C, D, E\}$ and $P_A^{3,d} = \{B, C\}$. And, $\neg DT_A^{1,d} = \{B, C, D, E\} - \{B, C, D\} = \{E\}$, $\neg DT_A^{2,d} = \{D, E\}$ and $\neg DT_A^{3,d} = \phi$. Then, $DF_A^{2,d} = \{D\}$, and $DF_A^{3,d} = \phi$, as shown in Fig. 4.

With $DT_i^{k,d}$ and $DF_i^{k,d}$ on each time slice, the disjoint time set DT_i of each trajectory TR_i in the query time interval T can be computed by Eq. 6 (The proof in Appendix A).

$$DT_i(T) = P_i - [(P_i - DT_i^{1,d}) \cup DF_i^{2,d} \cup \ldots \cup DF_i^{n,d}] \tag{6}$$

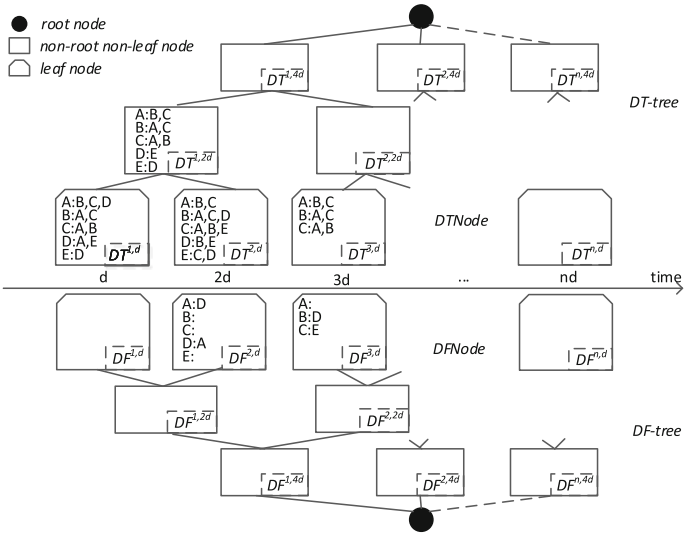

Fig. 4 DT-index

where $|T| = n \times d$, d is the length of the time slice, n represents the nth time slice, and P_i is a set which contains all trajectories that appear in T except the trajectory TR_i. For example, in Fig. 4, if $T = [0, 3d]$, $DT_D(T) = P_D^{0,3d} - [(P_D^{0,3d} - DT_D^{1,d}) \cup DF_D^{2,d} \cup DF_D^{3,d}] = \{A, B, C, E\} - [(\{A, B, C, E\} - \{E\}]) \cup \{A\} \cup \phi] = \{E\}$.

If T is too long, there are many time splices in T, and Eq. 6 contains many union operations of DF so that the computation of Eq. 6 is time-consuming. To alleviate the situation, we partition the time dimension into multiple levels of time slices. For instance, one level of time slices is a day, and another level is a week or month. So, if $|T|$ is one month, Eq. 6 can be computed by only one DF on the month level of time slices rather than by about 30 DFs on the day level.

(2) ***The structure of disjoint time index***

Based on the above analysis, we design the disjoint time index (called ***DT***-index) which includes a *DT-tree* and a *DF-tree* that saves the disjoint time set DT of each trajectory and its precomputation DF on different levels of time slices, respectively, as shown in Fig. 4. The two trees have the same structure. The *DT-tree* (*DF-tree*) consists of a single root node, leaf nodes, and non-root, non-leaf nodes. The detailed data structures of these nodes are as follows.

A root node, which may have multiple children, saves their *ID*s. As *ID* is both a time interval and a filename, when querying a time interval T, its children and their files are located quickly.

A leaf node stores pairs of $\langle i, DT_i \rangle$ or $\langle i, DF_i \rangle$ in a specific time slice. For example, in Fig. 4, $DT^{3,d}$ records pairs $\langle A, \{B, C\}\rangle$, $\langle B, \{A, C\}\rangle$ and $\langle C, \{A, B\}\rangle$.

A non-root, non-leaf node only has two children. It stores its children IDs and pairs of $\langle i, DT_i \rangle$ or $\langle i, DF_i \rangle$, where DT_i or DF_i can be computed by Eqs. 6 or 5, respectively.

For the DT-index, a bottom-up approach based on time slices is used to construct the DT-tree and the DF-tree. For each time slice on the bottom level, the leaf node $DT^{k,d}$ can be obtained by searching trajectories that meet the disjoint time constraint from B^+-tree. Then, the leaf node $DF^{k,d}$ is created by Eq. 5. If k is even, the content of its parent node (a non-root, non-leaf node) can be generated by Eqs. 6 or 5. In this order, non-root, non-leaf nodes in other levels in the two trees can be created. When the depth of the two trees reaches the limit, e.g., three levels of time slices, a root node is created based on its children.

Apparently, in order to obtain the disjoint time sets DT in T, a top-down traversal approach is used to find nodes whose time intervals are in T. Once it finds each of those nodes, it will omit searching its children and turn to search its siblings. The approach can obtain nodes whose time intervals are as long as possible. Since these found nodes may be in different levels while all operations in Eq. 6 are at the same level, Eq. 7 deduced from Eq. 6 is used to compute a final result based on different levels of time slices.

$$DT_i(T) = P_i - \{\underbrace{[(P_i - DT_i^{1,t_1}) \cup DF_i^{2,t_1} \cup \ldots\ DF_i^{n,t_1}]}_{l_1} \cup \underbrace{\ldots}_{l_2 \ldots l_{k-1}} \cup \underbrace{[(P_i - DT_i^{1,t_k}) \cup DF_i^{2,t_k} \cup \ldots\ DF_i^{n,t_k}]}_{l_k}\} \tag{7}$$

where l_i is a level of time slices.

For example, let $T = [0, 3d]$ and $P_A = \{B, C, D, E\}$, as shown in Fig. 4. Traversing in the DT-tree can obtain a node set $\{DT_A^{1,2d}, DF_A^{1,2d}, DT_A^{3,d}, DF_A^{3,d}\}$. According to Eq. 7, $DT_A(T) = P_A - \{[(P_A - DT_A^{1,2d}) \cup \phi] \cup [(P_A - DT_A^{3,d}) \cup \phi]\} = \{B, C\}$.

3.2 Processing query

With the B^+-*tree* and the DT-index, we implement an algorithm *QueryDTsTR* which quickly finds the disjoint time set DT of each trajectory and all sub-trajectories (denoted as *STRSet*) in a time interval T, as shown in Algorithm 1.

Algorithm 1: *queryDTsTR*

Input: B^+-*tree, DT-Index, T*
Output: *DT(T), STRSet*
1 $STRSet, DT(T_1), R(T_1), R(T_2),\ P$=*readsTR*($B^+$-*tree*, T) ;
2 $DT(T_2)$= *Equation* 7 ;
3 $DT = (DT(T1) \cup R(T_1)) \cap (DT(T2) \cup R(T_2))$;
4 return *DT*,*STRSet* ;

The query time interval T consists of two parts: One is a set of two time intervals without any time slices in the DT-index, denoted as $T_1 = \{t_1, t_2\}$; the other is the time interval that contains n time slices in the DT-index, denoted as T_2. For example, given $T = [8 : 35\ 11 : 25]$ and the minimal time slice is an hour, $T_1 = \{[8 : 35\ 9 : 00], [11 : 00\ 11 : 25]\}$, and $T_2 = [9 : 00\ 11 : 00]$. With the B^+-*tree*, it is easy to find all trajectories P and their sub-trajectories *STRSet* in T. Meanwhile, searching these sub-trajectories can obtain a trajectory set $R(T_1)$ where each trajectory appears in T_1 but not in T_2, a trajectory set $R(T_2)$ where each trajectory appears in T_2 but not in T_1, and a disjoint time set $DT(T_1)$ in the part T_1. The function *readSTR* at Line 1 implements the above process. Then, with the DT-index, the code at Line 2 computes the disjoint time set $DT(T_2)$ by Eq. 7. At last, the code at Line 3 gets the disjoint time set DT in T.

The algorithm can run very fast based on the following two reasons. One is that, in general, compared with the part T_2, the part T_1 is very short such that there are fewer sub-trajectories (*STR*s) in T_1. Hence, finding the disjoint time set $DT(T_1)$ is fast. The other is that, since the disjoint time set DT of each trajectory has been saved based on multiple timescales in the *DT*-index, only a small amount of nodes need to be searched from the index in order to compute the disjoint time set $DT(T_2)$ by Eq. 7. So, finding $DT(T_2)$ is also fast.

3.3 Splicing trajectory

3.3.1 Finding spliceable trajectories

We design an algorithm *createSTL-DAG* to discover spliceable trajectories by constructing a directed acyclic graph of sub-trajectory location connections (***STLC-DAG***), which is defined as *STLC-DAG* $= (V, E)$, where

- the vertex set V consists of all sub-trajectories (*STRSet*), a start vertex s, and an end vertex e, namely $V = \{STRSet\} \cup \{s, e\}$;
- the edge set E consists of two categories of directed edges. One, denoted as E_s, is the directed edge that connects two sub-trajectories in the same trajectory. The other, denoted as E_d, is the directed edge that connects a spliceable pair $\langle STR_i^j, STR_m^n \rangle$, as shown in Fig. 5.

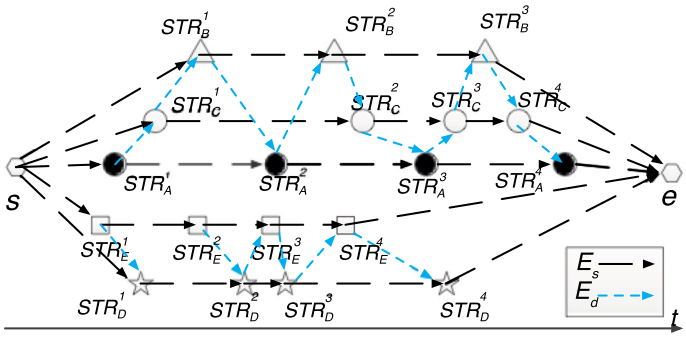

Fig. 5 *STLC-DAG*

According to the above definition of the graph *STLC-DAG*, edges in E_d, which represent spliceable pairs, are the key to determine whether two different trajectories can be spliced. However, if distances between any two sub-trajectories (vertexes) from different trajectories need to be computed, the process of constructing edges in E_d is slow. In order to speed up the process, if some edges in E_d cannot cause the result of splicing trajectories to change, these edges will be omitted according to Definition 6 and the following lemmas.

Definition 6 In the graph *STLC-DAG*, if there is a path, which is from the start vertex to the end vertex and contains all sub-trajectories of trajectories on the path, the path is called **spliced path**. Moreover, trajectories on the spliced path are **spliceable trajectories**.

In Fig. 5, the path, which passes through a vertex sequence $\langle s, STR_C^1, STR_B^1, STR_B^2, STR_C^2, STR_C^3, STR_B^3, STR_C^4, e\rangle$, is a spliced path, while the path $\langle s, STR_A^1, STR_C^1, STR_C^2, STR_A^3, STR_C^3, STR_C^4, STR_A^4, e\rangle$ is not a spliced path because it lacks the sub-trajectory STR_A^2. So, only trajectories on a spliced path can form a complete trajectory by the definition of the spliced path. Assuming all vertexes in the graph are sorted by their start time, the following lemmas can be deduced.

Lemma 1 *In the splice path sp, if there exists a directed edge between two sub-trajectories STR_i^j and STR_m^n from two different trajectories, there are not other sub-trajectories in the time gap between them, namely $ti(STR) \cap gap(STR_i^j, STR_m^n) = \phi$, where $STR \in sp$.*

Lemma 2 *Given two trajectories that meet the disjoint time constraint, if they are spliceable trajectories, there must be a path through all sub-trajectories from them in the graph STLC-DAG.*

Lemma 3 *Assuming the trajectory TR_i cannot splice with the trajectory TR_m, and the trajectory TR_m can be spliced with the trajectory TR_k, if TR_i and TR_k both are on a spliced path, the path must not contain sub-trajectories from the trajectory TR_m.*

The proofs of Lemma 1, 2, and 3 are omitted due to their simplicity. According to Lemma 2, in the process of constructing a spliced path, if the current vertex is the sub-trajectory STR_i^j, the next vertex that is selected to connect with STR_i^j must be the first sub-trajectory in the sequence of sub-trajectories, where all sub-trajectories belong to the same trajectory, and their time intervals are in the time gap between two sub-trajectories STR_i^j and STR_i^{j+1}.

Since there are the multiple sequences in the graph, all first vertexes from these sequences constitute a **candidate vertex set** (***CVS***), which is defined by Eq. 8.

$$CVS(STR_i^j) = \{STR_m^n | STR_m^n = first(\{ti(STR_m^k) \subset gap(STR_i^{j+1}, {}_m^k, STR_i^j)\}), m \in DT_i\} \tag{8}$$

For example, in Fig. 5, $CVS(STR_A^1) = \{STR_B^1, STR_C^1, STR_D^1, STR_E^2\}$.

Lemma 3 shows that when a trajectory cannot splice with another trajectory, the edges between the two trajectories can be deleted. Moreover, the deletion does not cause the result of spliceable trajectories to change.

The pseudocode of constructing the graph *STLC-DAG* is shown in Algorithm 2. The input arguments: the sub-trajectory set *STRSet* and the disjoint time set DT, are results of running the algorithm *queryDTsTR*, and γ is a distance threshold. The algorithm 2 will return a set $SP = \{SP_1, \ldots, SP_n\}$, where each SP_i is a group of spliceable trajectories.

Algorithm 2: *createSTLC-DAG*

```
   Input: STRSet, γ, SP = DT
   Output: SP
1  sortByStartTime(STRSet) ;
2  DAG.V = STRSet ∪ {s, e} ;
3  DAG.E_s = createEsEdge(STRSet, s, e) ;
4  C = φ ;
5  for k = 0; k < len(STRSet); k++ do
6      STR_i^j = STRSet[k] ;
7      for each STR_k^v ∈ sortByDes(C.get(STR_i^j)) do
8          sg = 0 ;
9          repeat
10             if !existPath(STR_k^v, STR_i^j, SP_k, DAG) then
11                 DAG.E_d.delEdges(TR_k, TR_i) ;
12                 SP_i = SP_i − k ;
13                 SP_k = SP_k − i ;
14                 C.del(⟨TR_i, TR_m⟩) ;
15                 sg = |C|;
16             else
17                 sg = sg − 1 ;
18             ⟨STR_k^v, STR_i^j⟩ ← C.next(STR_k^v, STR_i^j);
19         until ⟨STR_k^v, STR_i^j⟩ ≠ φ && sg > 0;
20     canTRSet = CVS(STR_i^j) ;
21     for each STR_m^n ∈ canTRSet do
22         if d(STR_i^j, STR_m^n) ≤ γ then
23             DAG.E_d.addEdge(STR_i^j, STR_m^n) ;
24         else
25             C.add(⟨STR_m^n, STR_i^j⟩) ;
26 return SP ;
```

Initially, the algorithm sorts all sub-trajectories in *STRSet* by their start time, creates all vertexes, and connects these vertexes that belong to the same trajectory (Line 1–3). C is a container that saves pairs of sub-trajectories which are likely to be indirectly spliced by

other sub-trajectories (Line 4). For each sub-trajectory STR_i^j in *STRSet*, its candidate vertex set $CVS(STR_i^j)$ is firstly obtained by Eq. 8. Then, the algorithm creates a directed edge between the two sub-trajectories STR_i^j and STR_m^n, where STR_m^n is from $CVS(STR_i^j)$, if the distance between the two trajectories is less than γ; otherwise, it adds the sub-trajectory pair $\langle STR_i^j, STR_m^n \rangle$ into the C (Lines 20–25) because they may be spliced indirectly.

The code on Lines 7–19 is used to decide whether the two sub-trajectories in the pair $\langle STR_k^v, STR_i^j \rangle$ from C can be spliced. If there is a path between them, it shows they may be spliced; otherwise, they cannot be spliced according to Lemma 2. So, delete all edges between the two trajectories that they belong to based on Lemma 3 (Line 11). Meanwhile, update their spliceable trajectory sets (Lines 12–13) and delete the pair from C (Line 14). The above deletion of edges causes a change in the path that connects two sub-trajectories from the pair in C so that the two sub-trajectories cannot be spliced. So, all pairs in C must be checked again. sg is a signal that represents whether all pairs have been checked or not. The function $nextPair$ returns next pair in C (Line 18).

The function $existPath$ (Algorithm 3) decides whether there is a path from the two sub-trajectory STR_k^v and STR_i^j (Line 10) by the depth-first search. If it finds the path, the path must be a spliced path according to Lemma 4 and 5.

Algorithm 3: *existPath*

Input: $STR_k^v, STR_m^n, SP_k, fCTR, DAG$
Output: $true$ *or* $false$
1 **if** $STR_k^v = STR_m^n$ **then**
2 return $true$;
3 $STR_k^v.marked = true$;
4 **for** *each* $STR_x^y \in DAG.neighbour(STR_k^v)$ **do**
5 **if** $(!\, STR_x^y.mark)$&& $(x \in SP_k \cup fCTR)$ **then**
6 $SP_k = SP_k \cap SP_x$;
7 $fCTR \leftarrow k$;
8 **if** $existPath(STR_x^y, STR_m^n, SP_k, fCTR, DAG)$ **then**
9 return $true$;
10 return $false$;

Lemma 4 *Assuming that Algorithm 2 is processing the current pair* $\langle STR_k^v, STR_i^j \rangle$*, the sub-trajectory* STR_i^j *is a temporary end vertex, and sub-trajectories from the same trajectory before trajectory* STR_k^v *constitute a temporary trajectory, if a path from* STR_k^v *to* STR_i^j *found by the function* $existPath$ *contains sub-trajectories from different temporary trajectories, these temporary trajectories can form a spliced path.* The proof is provided in "Appendix B".

When Algorithm 2 is processing an end pair $\langle STR_k^v, e \rangle$, a temporary trajectory equates a trajectory. So, if a path from STR_k^v to e found by Algorithm 2 contains different trajectories, these trajectories can form a spliced path. So, based on Lemma 4, it can easily deduce Lemma 5.

Lemma 5 *If and only if a path found by Algorithm 3 contains sub-trajectories from two different trajectories, the two trajectories can be spliced. The proof is provided in Appendix B*

After Algorithm 2 finishes its running, if there exists an edge between two trajectories in the graph *STLC-DAG*, the two trajectories can be spliced according to Theorem 1. At the same time, the algorithm can find groups of spliceable trajectories SP, where each SP_i is a set of trajectories that can be directly or indirectly spliced with the trajectory TR_i based on Theorem 2.

Theorem 1 *If there exists a directed edge between two trajectories in the graph STLC-DAG, the two trajectories can be spliced.*

Theorem 2 *For each $SP_i \in SP$, where SP is one of the output parameters of algorithm 2, SP_i is a set of trajectories that can splice with the trajectory TR_i.*

The above two proofs are provided in Appendix B.

3.3.2 Finding maximum spliceable trajectories

Definition 7 In the graph *STLC-DAG*, if no other spliced paths can contain a spliced path, the spliced path is called ***maximal spliced path***.

According to Definition 7, the trajectories on the maximal spliced path form a complete trajectory *CTR* which satisfies the trajectory splicing query according to Definition 5. With groups of spliceable trajectories (*SP*) obtained by Algorithm 2, we first create a ***SP***-set graph. Then, we demonstrate that a maximal clique in the graph is a maximal group of spliceable trajectories, and design an algorithm of listing all maximal cliques in order to get all complete trajectories.

The ***SP***-set graph (V, E), where $V = \{v | v = i, SP_i \in SP\}$ and $E = \{\langle i, j\rangle | j \in SP_i, SP_i \in SP\}$, can be created by *SP*. In the graph, vertex i represents the trajectory TR_i. SP_i is the set of neighbor vertexes of vertex i. Each edge shows that two vertexes are spliced with each other according to Theorem 2. Based on Lemma 6, a maximal clique in the graph is a complete trajectory *CTR*.

Lemma 6 *In the SP-set graph, a clique is a group of spliceable trajectories, and a maximal clique is a complete trajectory.* The proof is provided in Appendix B

We utilize a depth-first search algorithm (CLIQUES [34] to discover all complete trajectories. The algorithm can ensure to find all maximal cliques without duplications according to Theorem 1 of [34]. The detailed pseudocode is listed in Algorithm 4. The parameter *SUBG* denoted as Eq. 9 is a subgraph where each vertex is the trajectory that can splice with the trajectories on the spliced path *fCTR*.

$$SUBG = \left\{ i | i \in \bigcap_{s \in fCTR} SP_s \right\} \tag{9}$$

Let *CAND* be a set of remaining candidates in *SUBG*. At the initial stage, $SUBG = CAND = V$ and $fCTR = \phi$. The code on Line 2 finds a vertex i whose degree is a maximum in the subgraph $SUBG$. Owing to $max|SUBG \cap SP_i|$, $|CAND - SP_i|$ is minimal because $CAND \subseteq SUBG$. So, each branch in the depth-first search is minimal.

The operations $SUBG \cap SP_b$ and $CAND \cap SP_b$ (Lines 7–8) may lead to wrong spliced path because SP_b contains *TR*s that indirectly splice with TR_b. So, when the path *fCTR* is added into *fCTRSet*, *fCTR* must be checked by Definition 6 (Lines 11–13).

Algorithm 4: *findMaxCTR*

Input: $SP, SUBG = V, CAND = V, fCTR = \phi$
Output: *fCTRSet*: a *fCTR* set

```
if SUBG! = φ then
    i = subscript(max|SUBG ∩ SP_i|), i ∈ SUBG;
    branch = CAND − SP_i;
    while branch ! = null do
        b = takeFirst(branch) ;
        fCTR ← b;
        SUBG_b = SUBG ∩ SP_b;
        CAND_b = CAND ∩ SP_b;
        findMaxCTR(SP, SUBG_b, CAND_b, fCTR);
        CAND = CAND − {b};
else
    if isSplicePath(fCTR) then
        fCTRSet ← fCTR;
return fCTRSet;
```

3.3.3 Finding approximate maximal spliceable trajectories

Algorithm 4 can find complete trajectories (*CTR*s) as many as possible. But, its running time of the algorithm is exponential (Lemma 9 in Sect. 4). In practical applications, the maximum length of spliced paths can be known or predefined. For example, in the above case (Sect. 1), we can know how many systems capture trajectories. So, the number of spliceable trajectories on a spliced path must be less than(or equal to) the number of systems. Meanwhile, most of the practical applications can tolerate a maximal spliced path that contains a small number of wrong trajectories which cannot splice with another trajectory in the spliced path.

Therefore, we modify Algorithm 4 to discover spliced paths, where, in each path, the number of trajectories is no more than a predefined value ($\boldsymbol{d}$) under the condition that the probability of which a spliced path is a maximal splice path is more than a specific value ($\boldsymbol{p}$). Moreover, these spliced paths are called **approximate maximal spliced paths**.

According to Lemma 6, a maximal spliced path is a maximal clique in the *SP*-set graph. If the number of vertexes in the maximal clique is d, the number of edges in the maximal clique is $d(d-1)/2$. According to Eq. 9, the maximal spliced path can be obtained by executing $d-1$ intersections between SPs. If k intersections have been performed, $SUBG$ obtained by these intersections also can form a subgraph, where the number of edges is $\sum_{i=1}^{k+1}(d-i)$. The closer the number of edges in the subgraph is to $d(d-1)/2$, the more similar the subgraph is to the maximal clique. Therefore, the probability that the subgraph is a maximal clique is computed by Eq. 10.

$$p = \frac{\sum_{i=1}^{k+1}(d-i)}{d(d-1)/2} = \frac{(2d-k-1)k}{d(d-1)} \tag{10}$$

$$min(k) \;\; st. \;\; p \geq s \tag{11}$$

where k is the number of intersections; Eq. 11 represents the minimal number of intersections that satisfies the probability obtained by Eq. 10 which is greater than or equal to s. For example, if $d = 11$ and $p = 0.8$, $min(k) = 6$. If $d = 11$ and $p = 0.9$, $min(k) = 9$. Therefore, if a spliced path is obtained by computing k intersections, the probability that the spliced path is a maximal spliced path is more than p.

Algorithm 5: *findApproxMaxCTR*

Input: $SP, SUBG = V, CAND = V, d, k, c = 0, fCTR = \phi$
Output: *fCTRSet*:a *fCTR* set

```
1  if SUBG! = φ then
2      if c = k then
3          if |CAND| ≤ (d − k) then
4              fCTR ← CAND;
5          else
6              fCTR ← takeFirst(CAND, d − k);
7          fCTRSet ← fCTR;
8          return ;
9      i = subscript(max|SUBG ∩ SP_i|), i ∈ SUBG;
10     branch = CAND − SP_i;
11     while branch ! = null do
12         b = takeFirst(branch) ;
13         fCTR ← b;
14         SUBG_b = SUBG ∩ SP_b;
15         CAND_b = CAND ∩ SP_b;
16         fCTRSet = findApproxMaxCTR(SP, SUBG_b, CAND_b, d, k, c + 1, fCTR);
17         CAND = CAND − {b};
18 else
19     fCTRSet ← fCTR;
20 return fCTRSet;
```

Based on the above analysis, we design an algorithm *findApproxMaxCTR* to find approximate maximal spliced paths quickly. The detailed pseudocode of *findApproxMaxCTR* is listed in Algorithm 5. The algorithm is similar to Algorithm 4 except the code on Lines 2–8. The additional parameters are as follows: d, k, and c, where d is used to limit the number of spliceable trajectories in one complete trajectory; k, which is used to limit the time of intersection between two *SP*s, is a recursive depth of the algorithm; and c records the current time of computing intersections in a spliced path *fCTR*. The code on Lines 2–8 shows how to deal with trajectories in *CAND* when $c = k$. If the size of *CAND* is less than $d - k$, all trajectories in *CAND* are added into *fCTR* (Lines 3–4). If the size is more than $d - k$, the first $(d - k)$ trajectories are added into *fCTR* (Line 6).

4 Time complexity analysis

In this section, we quantify the running time of the above algorithms and ignore algorithms in the preprocessing step, such as the construction of B^+-tree and DT-index, because they can run offline. Let $\boldsymbol{T}$(*function*) be the running time of the *function*, M be the number of sub-trajectories, and N be the number of trajectories.

Lemma 7 *For the algorithm queryDTsTR, if the query time interval T consists of time slices from the DT-index, namely $T_1 = 0$ and $T_2 \neq 0$, the running time of queryDTsTR is $O(N^2)$; if the query time interval T does not contain the time slice for the DT-index, namely $T_2 = 0$ and $T_1 \neq 0$, the running time of queryDTsTR is $O(M^2)$.*

Proof Since all sub-trajectories are indexed by B^+-tree, the time of querying m sub-trajectories is $O(log_b^{|\Omega|} + M)$. $|\Omega|$ and b are constant. And, $log_b^{|\Omega|} \ll M$. So, the running

time of reading all sub-trajectories in T is $O(M)$. At the same time, $R(T_1)$ and $R(T_2)$ can be obtained. If $T_1 = 0$, $DT(T_1)$ does not need to be computed. Therefore, $T(readSTR) = O(M)$. If $T_1 \neq 0$, the running time of computing $DT(T_1)$ is $O(M^2)$. And, $T(readSTR) = O(M^2)$. If $T_2 = 0$, Eq. 7 does not need to be computed. So, $T(queryDTsTR) = O(M^2)$.

If $T_2 \neq 0$, given that T_2 consists of k time slices which are in different levels in DT-index, k nodes in the DT-index need to be read. Each node contains no more than N items in which there are at most N TRs. According to Eq. 7, T(Eq. 7)$= O(kN^2)$. The running time of intersection between $DT(T_1)$ and $DT(T_2)$ is $O(N^2)$. So, $T(queryDTsTR)$ is $O(N^2)$. □

Lemma 8 *The running time of the algorithm createSTLC-DAG is* $O(M^2N^2)$.

Proof Let $P = \sum_{i=1}^{N} |DT_i|$, where $DT_i \in DT$. So, $N \leq P \leq N^2$. The running time of creating vertexes (Line 3) and edges (Line 4) both are $O(M)$. In each loop (Line 5), $T(getCandSet) = O(m_k)$, where $m_k = |CVS(i, j)|$. And, the number of loops between Lines 21 and 25 also is m_k. $T(addEdge)$ and $T(add)$ both are $O(1)$. The number of creating all edges in E_d (Lines 20–25) is $\sum_{k=1}^{M} m_k$ since $len(STRSet) = M$. According to $CVS(STR_i^j)$ (Eq. 8), $m_k \leq DT_i$.

Since more sub-trajectories in TR_i result in less $|DT_i|$, the number of all edges is $\sum_{k=1}^{M} m_k$ and $\sum_{k=1}^{M} m_k \leq \frac{kM}{N} \times P$, where $k \ll N$. Moreover, running time of $pseudocode$ on Lines 20–25 is $O(\frac{M}{N} \times P)$. If all edges are added into DAG (Line 23), C is empty. If all edges are added into C (Line 25), the longest time that $existPath$ runs is $\frac{M}{N} \times P$ because $delEdges$ (Line 11) can delete some edges. $T(existPath)$ depends on the number of vertexes and edges between the two sub-trajectories STR_k^v and STR_m^n. So, $T(existPath) = O(M + \frac{M}{N} \times P)$. The running time of operations on Lines 11–17 all is $O(1)$. The running time of $pseudocode$ on Lines 5–19 is $O(\frac{M}{N} \times P \times (M + \frac{M}{N} \times P)) = O(\frac{M^2}{N} \times P + \frac{M^2}{N^2} \times P^2)$.

Thus, $T(createSTLC\text{-}DAG) = O(M + \frac{M}{N} \times P + \frac{M^2}{N} \times P + \frac{M^2}{N^2} \times P^2) = O(\frac{M^2}{N} \times P + \frac{M^2}{N^2} \times P^2) = O(\frac{M^2}{N} \times (P + \frac{P^2}{N}))$. Owing to $P \leq N^2$, $T(createSTLC\text{-}DAG) = O(M^2N^2)$ □

Lemma 9 *The running time of the algorithm findMaxCTR is* $O(3^{N/3})$.

Proof See Theorem 3 of [34]. □

Lemma 10 *Let D be a maximal degree of vertexes in the SP-set graph. The running time of the algorithm findApproxMaxCTR is $O(N(N-D)C_{k-1}^{D-1})$. Moreover, if k in Eq. 11 is a small numerical value, the running time of the algorithm findApproxMaxCTR is $O(CN^2)$, where C is a constant.*

Proof When the algorithm executes (depth 0) the code on Line 11 for the first time, $|branch| = N - D$. The algorithm will go to the branch SP_b, where the maximal degree of vertex b is D. Therefore, $|SUBG_b| \leq D$. When it executes (depth 1) the code on Line 11 for the second time, $|branch| \leq D-1$. When it executes the code on Line 11 for the third time, $|branch| \leq D-2$.

Each branch repeats the above process until the depth of iteration reaches k. As the depth increases, $|branch|$ decreases. Moreover, in depth $k-1$, $|branch| \leq D-k+1$. According to Theorem 1 of [34], the algorithm generates all maximal cliques without duplication. So, each branch in the depth 1 is looked at as a combination C_{k-1}^{D-1}. The running time of $SUBG \cap SP_i$ on Line 9 is $O(N)$. Thus, $T(findApproxMaxCTR) = O(N(N-D)C_{k-1}^{D-1})$. When k is small, C_{k-1}^{D-1} is also small. Then, $T(findApproxMaxCTR) = O(CN^2)$. □

Table 2 Parameters

Notation	Definition
γ	The threshold of the distance between *STR*s
d	The maximal length of a spliced path
p	Eq. 10
k	Top k complete trajectories (*CRT*s) sorted by Eq. 4

5 Experiments

In this section, we present the evaluation of the trajectory splicing query (Definition 5) and its algorithms based on two large real-world trajectory data sets. The first one is Geolife [47, 48], which is used to verify the effectiveness of our algorithms because it records labeled trajectories. The other is camera trajectory, which contains trajectories generated by the road safety cameras. Moreover, camera trajectory is mainly used to test the running time of algorithms, especially the algorithm *queryDTsTR* based on the DT-index, because it has large amounts of trajectories.

We use the two algorithms *findMaxCTR* and *findApproxMaxCTR* to implement the trajectory splicing query, respectively. Moreover, we implement the above two algorithms in Java language on a Linux server with Intel Xeon quad-core and 8 GB of main memory. The parameters used in the following experiments are defined in Table 2.

5.1 Evaluation on geolife

5.1.1 Data set and parameter setting

In the experiment, we extract trajectories from GeoLife in 2008 as the test dataset. This test dataset contains 4405 trajectories from 32 users. Each segment of those trajectories has been labeled by one of 11 transportation modes, which are bike, boat, bus, car, run, subway, taxi, train, walk, airplane, and others. These segments are considered from 11 different datasets. So, segments from the same user with the same label make up the trajectory defined in the paper, denoted as *TR*. Each segment is the sub-trajectory defined in the paper, denoted as *STR*. The test dataset contains 138 *TR*s and 4405 *STR*s, listed in Table 3.

The function $dist(i, j)$ is the Euclidean distance between two *TR*s with two labels i and j, respectively. Table 4 lists maximum, mean, and variance of $dist(i, j)$. For example, the first row in Table 4 represents the mean, variance, and max distance between bike-*TR*s and other-*TR*s, which are 109,477 m, 146,006 m, and 212,719 m, respectively. We set four values

Table 3 Composition of *TR* Datasets

Id	Dataset	*TR*	*STR*	Id	Dataset	*TR*	*STR*
1	Airplane	1	2	7	Subway	7	108
2	Bike	14	301	8	Taxi	13	71
3	Boat	1	1	9	Train	4	12
4	Bus	22	426	10	Walk	28	756
5	Car	16	337	11	Other	30	2383
6	Run	2	8				

Table 4 Mean, Variance and Max in $dist(i, j)$

Dist	*Mean* (m)	*Var* (m)	*Max* (m)	*Dist*	*Mean* (m)	*Var* (m)	*Max* (m)
1, 11	109, 477	146, 006	212, 719	4, 9	133, 446	173, 046	255, 808
1, 4	14, 576	0	14, 576	5, 10	55, 642	328, 973	2, 415, 622
1, 8	293, 078	0	293, 078	5, 11	34, 362	118, 063	1, 063, 245
2, 10	1500	2777	12, 075	5, 7	8564	39, 313	267, 034
2, 11	11, 257	84, 761	1, 023, 086	5, 8	11, 348	20, 908	76, 762
2, 4	2549	3654	12, 689	5, 9	13, 957	0	13, 957
2, 5	10, 001	17, 305	52, 276	7, 10	5850	7080	31, 996
2, 7	13, 171	20, 661	44, 042	11, 7	41, 265	132, 648	637, 270
2, 8	58, 703	118, 024	269, 712	7, 8	2265	4143	11, 631
3, 4	59, 156	73	59, 207	8, 10	15, 221	26, 122	77, 098
4, 10	12, 583	84, 028	986, 741	11, 8	223, 333	1, 214, 825	8, 328, 956
4, 11	23, 340	110, 415	1, 066, 120	8, 9	761, 691	951, 360	1, 828, 952
4, 5	124, 336	548, 462	2, 517, 981	9, 10	66, 511	98, 627	235, 890
4, 6	601	1315	5516	11, 9	468, 275	466, 053	1, 245, 493
4, 7	5894	11, 273	56, 182	11, 10	20, 986	109, 772	1, 125, 060
4, 8	6966	18, 875	77, 229				

for the parameter γ, which are $\gamma = m$, $\gamma = m + v$, $\gamma = m + 1.5v$ and $\gamma = max$, where m, v, and max are *mean*, *var*, and *max* in Table 4, respectively.

5.1.2 *findMaxCTR* vs *findApproxMaxCTR*

In order to evaluate the effectiveness of the two algorithms that splice trajectories from the above 11 datasets, we define ***recall***, ***precision***, and ***completeness*** as Eqs. 12, 13, and 14. $recall$ represents the ability of which the two algorithms can recover complete trajectories (*CTR*) from the above 11 datasets; *precision* can show the degree of which top k *CTR*s contain user trajectories in Geolife; *completeness* is the degree that one complete trajectory recovers a user trajectory.

$$recall = num_a / num_b \tag{12}$$

where num_b is the number of user trajectories in the test dataset and num_a is the number of user trajectories found by one of the two algorithms. In this experiment, $num_b = 32$ due to total 32 user trajectories in the dataset.

$$precision = num_c / k \tag{13}$$

where num_c is the number of complete trajectories that contain a user trajectory; k refers to top k complete trajectories ranked by Eq. 4.

$$completeness = \frac{|label(CTR) \cap (userTra)|}{|label(userTra)|} \tag{14}$$

where the function $label(.)$ returns the set of transportation modes in a trajectory; $|label(userTra)|$ is the number of labels that appear in a user trajectory *userTra* in the dataset; and $|label(CTR) \cap label(userTra)|$ is the number of labels that appear both in *CTR* and *userTra*.

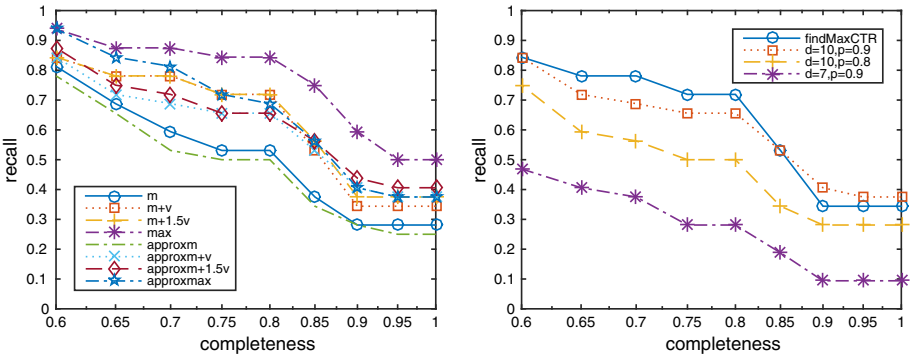

(a) Max vs Approx recall on diff γ **(b)** Max vs Approx recall on m+v

Fig. 6 *findMaxCTR* versus *findApproxMaxCTR* on *recall*

The *recall* results of *findMaxCTR* and *findApproxMaxCTR* that run on different γs are shown in Fig. 6a, where m, $m + v$, $m + 1.5v$, and max are four parameter values for γ. The first four curves are results of *findMaxCTR*, and the last four curves are results of *findApproxMaxCTR*. Apparently, the higher the *completeness*, the lower the *recall*. With increasing γ, *recall* rises because the two algorithms can find more complete trajectories. For example, as shown in Fig. 7a, *findMaxCTR* found 44,002 complete trajectories at $\gamma = mean$, and 2,018,701 complete trajectories at $\gamma = max$. So, the running time of the two algorithms becomes slow when $gamma$ increases. The running time of *findMaxCTR* is 14 s on $\gamma = mean$ while 427 s on $\gamma = max$.

The *recall*s of the two algorithms that run on $\gamma = mean + var$ are shown in Fig. 6b. In general, *findMaxCTR* can find more user trajectories than *findApproxMaxCTR*. However, as the parameters d or p become large, *findApproxMaxCTR* can find more user trajectories than *findMaxCTR*. This is because *findApproxMaxCTR* is an approximate algorithm of *findMaxCTR*, and according to Eq. 10, the larger the parameters d or p, the larger the parameter k (the number of intersection in the SP-set graph), and the more likely it is to obtain clique in the graph. Thus, *findApproxMaxCTR* is more similar to *findMaxCTR*. Moreover, owing to its proximity, *findApproxMaxCTR* ignores the certain restrictions on the parameter $gamma$ and the disjoint time condition so that it can discover more user trajectories.

The running time of *findMaxCTR* versus *findApproxMaxCTR* on $\gamma = m + v$ is illustrated in Fig. 7b. *findApproxMaxCTR* runs faster than *findMaxCTR* because the time complexity of *findApproxMaxCTR* is $O(CN^2)$ while $findMaxCTR$ is $O(3^{N/3})$. The time of *findApproxMaxCTR* running on three groups of parameters, ($d = 10$, $p = 0.9$), ($d = 10$, $p = 0.8$), and ($d = 7$, $p = 0.9$), are 2.4s, 1.8s, and 1.6s, respectively, because the recursion depths of *findApproxMaxCTR*, according to Eq. 11, are 7, 6, and 5, respectively. Moreover, the number of complete trajectories found by *findApproxMaxCTR* decreases as the recursion depth becomes smaller.

The *precision* results of the two algorithms on different k values are shown in Fig. 8, where *findApproxMaxCTR* runs with $d = 10$ and $p = 0.9$. Smaller or bigger γ is bad to promote *precision* because smaller γ results in lower *recall*; bigger γ incurs more complete trajectories. On GeoLife, when $\gamma = m + v$ or $\gamma = m + 1.5v$, the precision of *findApproxMaxCTR* is better.

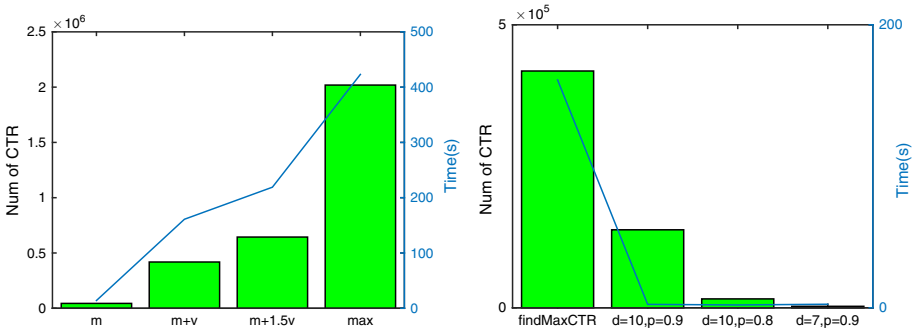

(a) findMaxCTR time(s) **(b)** Max vs Approx time($\gamma = m + v$)

Fig. 7 *findMaxCTR* versus *findApproxMaxCTR* on $time$

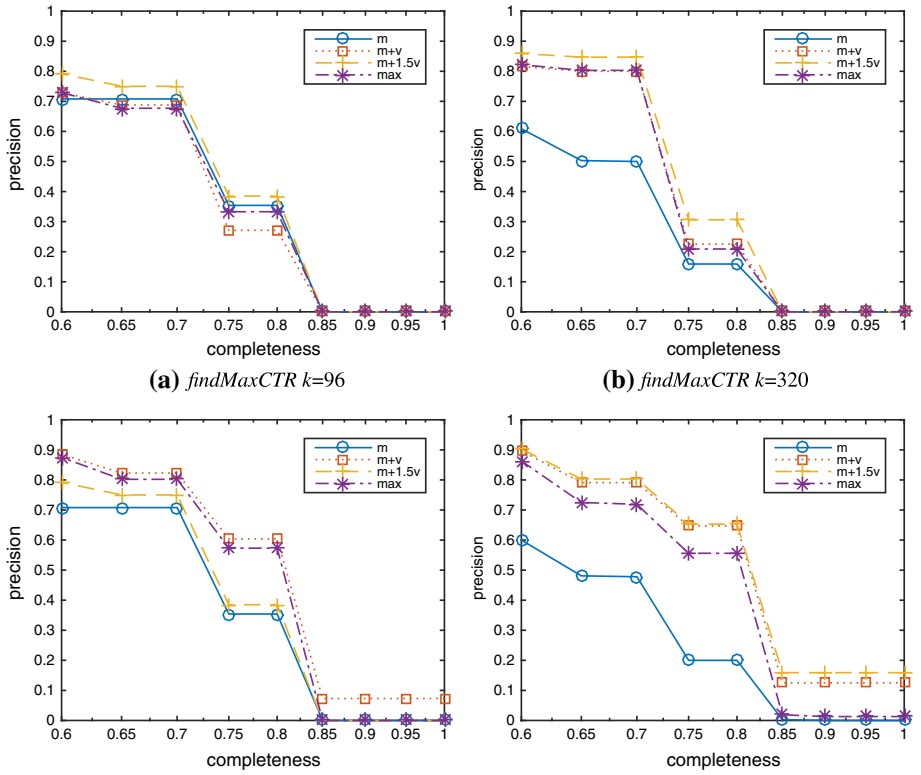

(a) *findMaxCTR* k=96 **(b)** *findMaxCTR* k=320

(c) *findApproxMaxCTR* k=96 **(d)** *findApproxMaxCTR* k=320

Fig. 8 *precision* of *findMaxCTR* and *findApproxMaxCTR* on different k

Compared with *findMaxCTR* on $\gamma = m + v$, as shown in Fig. 9, *findApproxMaxCTR* with $d = 10$ and $p = 0.9$ or $p = 0.8$ has higher *precision* because these approximate *CTR*s found by *findApproxMaxCTR* are robust so that they can contain more right user trajectories.

According to the F1 scores with considering $recall$ and $precision$, as shown in Fig. 10, *findApproxMaxCTR* surpasses *findMaxCTR* on the GeoLife dataset. This is because the *recall*

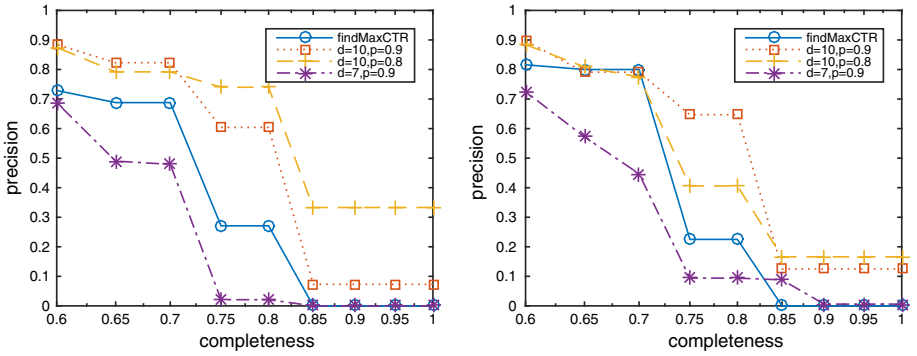

(a) k=96 **(b)** k=320

Fig. 9 *precision* of *findMaxCTR* versus *findApproxMaxCTR* on $\gamma = m + v$

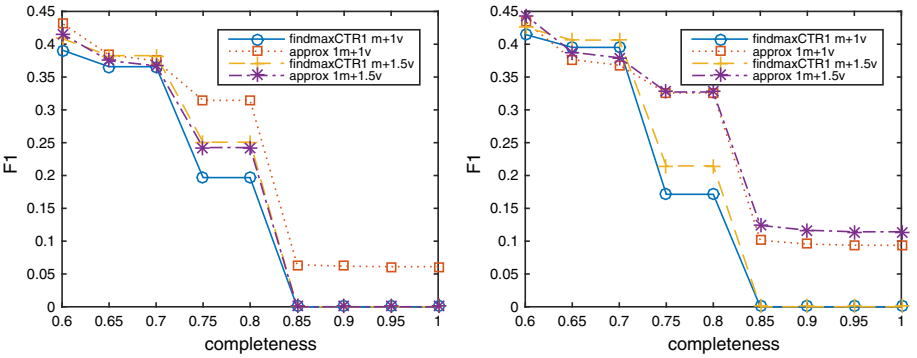

(a) k=96 **(b)** k=320

Fig. 10 F1 score of *findMaxCTR* versus *findApproxMaxCTR*

of *findApproxMaxCTR* is close to that of *findMaxCTR*, while the $precision$ of *findApproxMaxCTR* is much larger than that of *findMaxCTR*.

5.1.3 Comparison with the fuzzy trajectory linking method

Compared with our algorithms, the most similar work is the fuzzy trajectory linking method (FTL) [38] which links two trajectories and evaluates whether they can be spliced with each other with a certain probability. We choose *findMaxCTR*($\gamma = m + v$ and $speed < 200$ km) and naïve-Bayes-matching algorithm (***nbayes***, $\phi_r = 0.9$, and $speed < 200$ km) from FTL to recover user trajectories from any two of the three datasets: walk, bus, and car. If a user trajectory consists of two trajectories with the same personal ID, the user trajectory is called **right trajectory**. The number of right trajectories recovered by the two algorithms is illustrated in Fig. 11. *findMaxCTR* can find all right trajectories, while *nbayes* omits some of them because FTL cannot describe all spliceable features between two trajectories with the Poisson–Binomial distribution whose assumption is that random samples are independent and identically distributed (i.i.d). Trajectories from different datasets do not meet the condition of i.i.d.

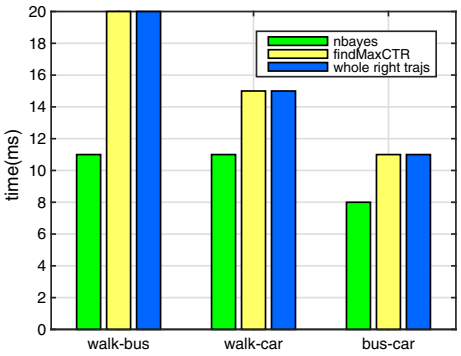

Fig. 11 *nbayes* versus *findMaxCTR* on right trajectories

5.2 Evaluation on CameraTrajectory

5.2.1 Data set and parameter setting

In the dataset, a trajectory consists of sample points that are generated by road safety cameras, which record information of vehicles that pass by them. The dataset has 10,104 trajectories and 12,741,728 sample points over three months at Guyuan, China. Since we do not know which trajectories in the dataset can be spliced in advance, for computing effectiveness of the algorithm, we manually select 104 trajectories from the dataset as test trajectories and randomly split these trajectories into 568 trajectories. After the two algorithms run, we observe how many complete trajectories (*CTR*s) contain these test trajectories. Thus, we can compare *recall*, *precision*, and F_1 between the two algorithms. By setting thresholds $speed = 1$ (m/s) and $distance = 10{,}000$ (m), all trajectories in the dataset are split into sub-trajectories. So, there is a total of 10,568 trajectories (*TR*s) and 1,812,568 sub-trajectories (*STR*s) in the dataset.

5.2.2 *findMaxCTR* vs *findApproxMaxCTR*

With the parameter $\gamma = 5000$ m, the results of *findMaxCTR* versus *findApproxMaxCTR* are shown in Fig. 12, where ($d = 7$, $p = 0.9$), ($d = 14$, $p = 0.9$), ($d = 28$, $p = 0.9$), and ($d = 38$, $p = 0.9$) are the four groups of parameters in *findApproxMaxCTR*. *findMaxCTR* finds total 13,581 groups of spliceable trajectories. However, its *recall* is about 20% as shown in Fig. 12a, because many spliceable trajectories found by it do not satisfy the function *isSplicePath* so that they are discarded.

Compared with *findMaxCTR*, *findApproxMaxCTR* finds approximate maximal spliceable trajectories which are not checked by *isSplicePath*. Therefore, it has a higher *recall* than *findMaxCTR* when d is bigger. For example, when $d = 38$ and $p = 0.9$, its *recall*s are 82% on *completeness* $= 1$ and 93% on *completeness* $= 0.85$, respectively. However, when $d = 7$, it has a lower *recall* because the code on Lines 2–8 prunes many branches that contain spliceable trajectories in Algorithm 5. So, if d is in a reasonable range, *findApprox-MaxCTR* is more robust than *findMaxCTR* because its approximate results are not filtered by Definition 5.

When selecting the first 4000 results found by the two algorithms, the precisions of the two algorithms are illustrated in Fig. 12b. Compared with *findApproxMaxCTR*, *findMaxCTR* can find more user trajectories although it has a poor ability to find user trajectories with high

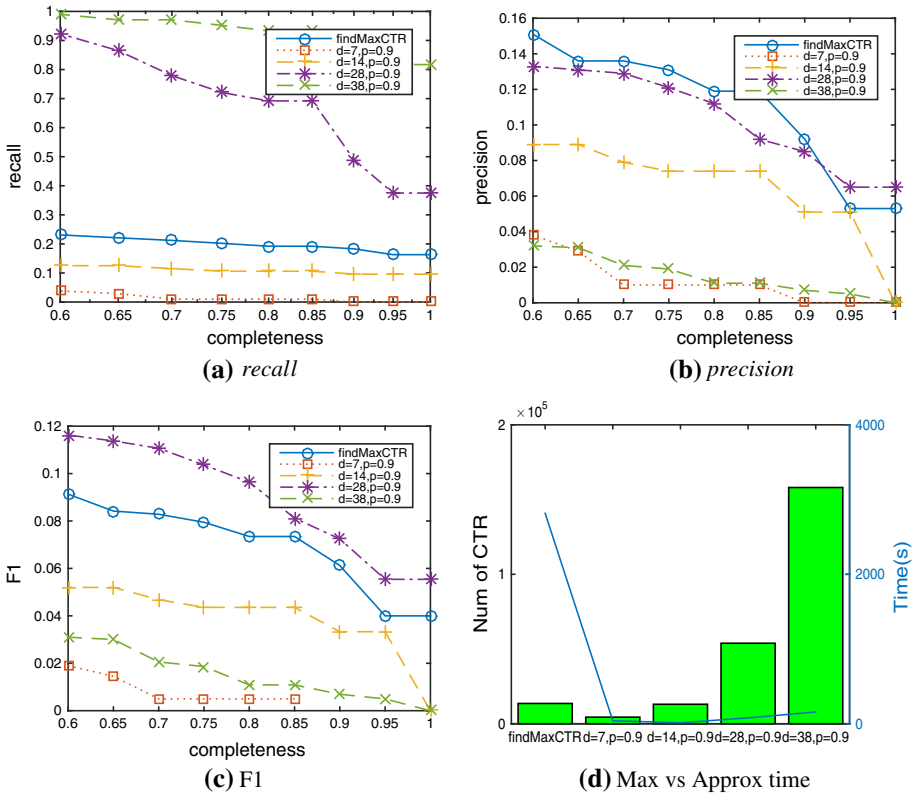

(a) *recall* **(b)** *precision*

(c) F1 **(d)** Max vs Approx time

Fig. 12 $findMaxCTR$ versus $findApproxMaxCTR$

completeness. According to the F1 scores on Fig. 12c, *findApproxMaxCTR* with the fitted parameters ($d = 28$ and $p = 0.9$) is better than *findMaxCTR*. However, searching for the right parameter values is very troublesome since it needs to try many different parameter values. So, from the view of simplicity, *findMaxCTR* is a good choice.

The time of *findMaxCTR* running on GeoLife (138 *TR*s) is about 160s, while its time on CameraTrajectory (10568 *TR*s) is about 2816s, as shown in Figs. 7b and 12d. However, its running time does not follow the exponential growth as its time complexity $O(3^{N/3})$, because the density[2] of the *SP*-set graph is 0.56 on GeoLife while it is 0.0054 on CameraTrajectory. Moreover, the running time of listing maximal cliques also depends on the density of the graph. In Fig. 12d, with different parameter values, the time of *findApproxMaxCTR* running on CameraTrajectory is about 13 s, 40 s, 79 s, and 157 s, respectively. Its time is almost the same because it runs much time on *createSTLC-DAG* whose time complexity is $O(M^2N^2)$, while it runs a minimal amount of time on the step of finding approximate maximal spliced path since the *SP*-set graph is very sparse (its density is 0.0054).

5.3 Evaluation on *DT*-index

A B^+-tree and a *DT*-index are built on CameraTrajectory to evaluate their efficiencies of querying disjoint time sets. The length of the minimal time slice is 8 days. In *DT*-index, the

[2] https://en.wikipedia.org/wiki/Dense_graph.

Table 5 Components in DT-tree

Level	DT-tree		DF-tree	
	# of *DTNode*	*Avg size*(*kb*)	# of *DFNode*	*Avg size*(*kb*)
1	13	39,002	12	33,124
2	6	39,831	5	43,695
3	3	37,905	2	87,141

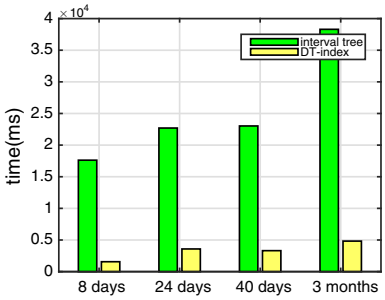

Fig. 13 B^+-tree versus DT-index on computing DT

DT-tree and the DF-tree both have three levels of nodes except their rood nodes. The sizes of the B^+-tree and the DT-index are 137 Mb and 1.65 Gb, respectively, after constructing the two indexes. Table 5 lists the details of the DT-index. The sizes of *DTNode*s in different levels are almost the same because, according to Eq. 15, longer the time, smaller the change in the disjoint time set of a trajectory. However, the change of sizes between *DFNode*s at different levels is big, because there is a significant difference between the two neighboring $\neg DT_i$s so that the size of DF_i is large based on $DF_i^n = \neg DT_i^n - \neg DT_i^{n-1}$. Although the size of the DT-index is very large, some lossless data compression algorithms, e.g., LempelZiv(LZ) compression algorithm, can decrease its size. By $LZ78$ algorithm, the size of the DT-index changes from 1.65 Gb to 700 Mb.

As mentioned earlier in *queryDTsTR*, if $T_2 = 0$, it will search the disjoint time sets of all trajectories in the B^+-tree (called ***ITQuery***). If $T_1 = 0$, it will search all the disjoint time sets in the DT-index (called ***DTQuery***). After *ITQuery* and *DTQuery* run 10 times in different time intervals (8, 24, 40 days, and 3 months), their average time is shown in Fig. 13.

Apparently, *DTQuery* runs faster than *ITQuery* because the time complexity of *DTQuery* is $O(N^2)$ while the time complexity of *ITQuery* is $O(M^2)$, and $M \gg N$. As the query time grows, M becomes bigger but N does not change. So, the main factor that affects the running time of *DTQuery* is only the I/O time of reading the disjoint time set from the DT-index while the main factors that affect *ITQuery* include the time of reading trajectories from the B^+-tree and the time of computing the disjoint time sets in CPU.

6 Related work

6.1 Trajectory indexing and querying

In the paper, to find trajectories whose times are disjoint quickly, it needs to search for trajectories according to the time intervals between their sub-trajectories. The interval tree [14],

which is built based on the time, supports to retrieve sub-trajectories in these time intervals. Moreover, the indexes based on B^+-tree [37] and R-tree [18,33,35,40] can efficiently process the query of time intervals. Although these indexes can process the query, they cannot efficiently deal with the query of time-disjoint sets because, in each query, they only support to search in a specific time interval not in multiple time intervals so that they need many queries of time intervals to discover these trajectories whose times are disjoint.

In addition to the disjoint time constraint on trajectories, spliceable trajectories require that the gap distances between them are close enough that they constitute a complete trajectory. Symbolic trajectories [13], which gives us a conceptual view to understand various behaviors of the moving object [30], can capture these spliceable trajectories by a sequence of time-dependent labels. The symbolic trajectory of a moving object is represented as a sequence of units $\langle u_1, u_2, \ldots, u_n \rangle$, where u_n is a pair $\langle t, s_b, s_e, l \rangle$ in which i is a time interval, s_b and s_e are the locations of two endpoints of the unit, and l is a label. For example, for the case in Sect. 1, the symbolic trajectory of Bob is the sequence $\langle([8:00-8:20], H, A, walk), ([8:23-9:14], A, B, subway), ([9:16-9:21], B, C, walk), \ldots\rangle$.

Güting et al. [13,29,35,40] create the data model of symbolic trajectories and their indexes to offer operations to search trajectories by the above sequence of time-dependent labels. More specially, these operations support to retrieve symbolic trajectories which satisfy the condition of the time interval, spatial distance, and a sequence of labels. For example, the retrieval SQL of Bob transitions from walk to subway is "$select\ pid\ from\ Case1\ where\ trans\ matches'*X(\_walk)\,Y(\_subway)*//\,Y.start-X.end \leq duration(0\,9000000)'\ and\ pid = Bob$". In order to match the symbolic trajectory from the database, the query must know the sequence of labels in advance. However, in the paper, the sequence of $label$ is unknown before the query begins to retrieve spliceable trajectories. So, symbolic trajectory methods do not apply to queries for the spliced mode.

Spatiotemporal joins [32,49] find close pairs of trajectories from two datasets, respectively, based on the distance between the pair of trajectories. Based on these close pairs, the trajectory join [1] retrieves groups of moving objects that have similar movements at a different time. Kexin Xie et al. [39] propose a spatiotemporal join method to associate segments of a trajectory with points of interest (POI) according to the distance between a POI and a trajectory and duration which a trajectory is geographically near a POI. However, the distances in these spatiotemporal join methods are the similarity between the two trajectories, while the gap distance between two trajectories is the Euclidean distance. So spatiotemporal joins are not fit to find spliceable trajectories defined in this paper because these spliceable trajectories are not similar.

6.2 Trajectory pattern analysis and mining

The spliced model needs to find groups of spliceable trajectories from different systems. Group pattern mining and trajectory clustering both find groups of moving objects based on similarity of their trajectories in a specific time interval, such as flock [8,9,36], convey [19], swarm [27], group [26], gathering [45], and trajectory clustering methods [24,25]. These methods define different distance functions to evaluate the similarity between trajectories, and design corresponding cluster algorithms to discover groups of similar trajectories. However, these methods are not fit to find groups of spliceable trajectories because they find similar trajectories while spliceable trajectories are not similar. Another line of research on frequent trajectory mining targets at assigning travel cost-based weights to edges [15,16,42] and paths [3,44] that are frequently traversed by trajectories, where the travel costs can be travel

time or fuel consumption [11,12]. However, only frequently traversed edges and paths are identified, which cannot be used directly to identify spliceable trajectories.

From the view of recovering complete user trajectories, a spliceable trajectory is one of the transportation modes in the user complete trajectory. So, discovering spliceable trajectories needs to decide whether other trajectories can splice with the current trajectory based on their information about time, location, and transportation mode. Trajectory inference methods [5, 28,31,46] seem to be able to make the above decision since these methods can predict a user's location, infer his transportation mode, and predict when and where he will change modes [28] based on the known trajectory information. However, these methods are not good at dealing with the problem of splicing multiple trajectories owing to the two following reasons. One is that the problem of trajectory splicing act on the different data sources while trajectory inference methods act on a single data source. In multiple data sources, each data source has a different ID code and contains trajectories of one transportation mode, and it is difficult to know in advance whether trajectories from different data source belong to a user movement. So, the model of the problem is not built on a user history trajectory. More specifically, it is impossible to count the probability that one user switches one transportation mode to another. But, a single data source makes trajectory inference methods know user complete trajectory so that they can create their models based on user history trajectory.

The other is that they have different goals. The goal of our work is to match trajectories so that they can form one group, while the goal of trajectory inference methods is to predict a user's location, infer his transportation mode, and so on. From the view of statistical learning, our work is the clustering problem, while trajectory inference methods are the regression problem. Preference learning is able to identify driver groups with similar driving preferences and thus group their trajectories together [2,12,43]. However, it is unable to identify individual drivers.

The fuzzy trajectory linking(FTL) [38] is close to our work. It finds pairs of trajectories that belong to the same moving object by the two methods: (α_1, α_2)-filtering and naïve Bayes matching. Compared with our methods, FTL can link (splice) two trajectories based on the distribution of distances between any two time-order points from the two trajectories, respectively. So, it avoids the disjoint time constraint in our work so that it can splice two trajectories even if their sub-trajectories overlap with each other in time. However, it does not support multiple trajectories splicing efficiently because the two above methods will be invalid as more trajectories are involved in a spliced process. Nevertheless, our methods can splice multiple trajectories. Driver identification is also similar to our work in the sense that it also tries to identify trajectories from different drivers. However, it focuses on learning distinctive representations of driving behaviors and then clusters the representations [20], but ignores disjoint time and spatial closeness.

7 Conclusion

In this paper, we study the problem of trajectory splicing, which reconstructs individual complete trajectories which enables to analyze holistic behaviors of individual moving objects. To content with the challenge that searching trajectories whose time intervals are disjoint is very time-consuming, we propose the DT-index to improve the search efficiency. In addition, we propose two algorithms: *findMaxCTR* and *findApproxMaxCTR* to discover spliceable trajectories. Our experiments based on two real trajectory databases demonstrate the two algorithms are able to solve the problem efficiently.

For future work, it is of interest to extend the spliced degree by considering other factors, such as the number of the sub-trajectories, and the shape of the sub-trajectories, to evaluate the quality of the reconstructed individual complete trajectory. It is also of interest to parallelize [41] the proposed algorithms to improve the efficiency and to relax the time-disjoint constraint to extend the spliced model to include more individual partial trajectories.

Acknowledgements We would like to thank Professor Christian S. Jensen for useful discussions and comments. This work was supported by National Science and Technology Major Project (no. 2017ZX05018-005), National Natural Science Foundation of China (no. 61402532), Science Foundation of China University of Petroleum-Beijing (no. 01JB0415), and China Scholarship Council.

Appendix A Computing disjoint time set

Lemma *In the query interval time T, the disjoint time set DT_i of each trajectory TR_i can be computed by Eq. 6.*

Proof Let $Q_i^{k,d}$ be a trajectory set where each trajectory TR appears in T and its time interval set $ti(TR)$ does not overlap with TR_i in the kth time slice. So, $Q_i^{k,d} = DT_i^{k,d} \cup R^{k,d}$, where $R^{k,d}$ is a trajectory set in which each trajectory appears in T except in the kth time slice. For example, in Fig. 2, assumed $T = [0, 3d]$, $R_A^{3,d} = \{D, E\}$ and $DT_A^{3,d} = \{B, C\}$. Then, $Q_A^{3,d} = \{B, C, D, E\}$. Therefore,

$$DT_i(T) = Q_i^{1,d} \cap Q_i^{2,d} \cap \ldots \cap Q_i^{n,d} \tag{15}$$

Due to $P_i = P_i^{1,d} \cup P_i^{2,d} \cup \ldots \cup P_i^{n,d}$,

$$\neg DT_i^{k,d} \cup Q^{k,d} = P_i \tag{16}$$

$$\neg DT_i^{k,d} \cap Q_i^{k,d} = \phi \tag{17}$$

According to Eqs. 5, 16 and 17, Eq. 15 can be deduced as follows.

$$\begin{aligned} DT_i(T) &= (P_i - \neg DT_i^{1,d}) \cap \ldots \cap (P_i - \neg DT_i^{n,d}) \\ &= P_i - [\neg DT_i^{1,d} \cup (\neg DT_i^{2,d} - \neg DT_i^{1,d}) \\ &\quad \cup \ldots \cup (\neg DT_i^{n,d} - \neg DT_i^{n-1,d})] \\ &= P_i - [(P_i - DT_i^{1,d}) \cup DF_i^{2,d} \cup \ldots \cup DF_i^{n,d}] \end{aligned} \tag{18}$$

□

Appendix B Finding spliced trajectory

Lemma 4. Assuming that Algorithm 2 is processing the current pair $\langle STR_k^v, STR_i^j \rangle$, the sub-trajectory STR_i^j is a temporary end vertex, and sub-trajectories from the same trajectory before trajectory STR_k^v constitute a temporary trajectory, if a path from STR_k^v to STR_i^j is found by the function $existPath$, temporary trajectories that the path have passed through can form a spliced path.

Proof Let P_c which is found by *existPath* be a path from STR_k^v to STR_i^j. We firstly prove there must exist a path P_l from STR_k^v to STR_i^j in the current graph *STLC-DAG*. P_l is an time-ordered sequence where each $STR \in \{STR_m^n | ti(STR_k^v).st < ti(STR_m^n).st < ti(STR_i^j).st, m \in M(P_c)\} \cup \{STR_k^v, STR_i^j\}$. And, $M(P_c)$ is a set of *TR*s that P_c have passed through except i and k. We prove the problem according to the following situations.

If $|M(P_c)| = 0$ or $|M(P_c)| = 1$, P_c must be P_l.

If $|M(P_c)| \geq 2$, suppose P_l does not exist in the current *STLC-DAG*. Let P_a be the path contains the maximum number of *STR*s from P_l, where $M(P_c) \subseteq M(P_a)$. Then, at least one vertex STR_m^n from P_l is not on P_a. According to time, let STR_m^n be between $P_a[i]$ and $P_a[i+1]$, namely $ti(P_a[i]).st < ti(STR_m^n).st < ti(P_a[i+1]).t$, where $P_a[i](P_a[j])$ is a ith or jth *STR* in P_a, $m_i(m_{i+1})$ is the subscript of $P_a[i](P_a[i+1])$, and $m_i, m_{i+1} \in m(P_c)$. Therefore, before running the current pair, the algorithm has executed evaluation of the two pair $\langle P_a[i], STR_m^n \rangle$ and $\langle STR_m^n, P_a[i+1] \rangle$. The evaluation generated two following results. One is that, if there does not exist a path between $\langle P_a[i], STR_m^n \rangle$ or $\langle STR_m^n, P_a[i+1] \rangle$, it shows TR_m and $TR_{m_i}(TR_{m_{i+1}})$ cannot be spliced. So, $m_i \notin SP_m$ or $m_{i+1} \notin SP_m$. According to $existPath$ (Algorithm 3), it cannot find that a path contains $STR_{m_i}(STR_{m_{i+1}})$ and STR_m. It contradicts with P_c. The other is that, if there does exist both above paths, STR_m^n can be added into P_a. It contradicts with P_a that has the maximum number of *STR*s from P_l. Therefore, P_l must exist in the current *STLC-DAG*.

Then, since P_l from STR_k^v to STR_i^j exists in *STLC-DAG*, it implies that there must exists a path P_b from the start vertex to STR_k^v in the current *STLC-DAG*. And, P_b contains all *STR*s of *TR*s between the start vertex and $STR_k^v(P_c$ has passed through these *TRs*). This is because the algorithm has processed previous pair $\langle STR_t^r, STR_k^v \rangle$. And, there must exist a path P_t similar to P_a between STR_t^r and STR_k^v owing to the path found by *existPath*. And so on, these previous pairs form the P_b. Therefore, the P_b and P_l can form a spliced path. □

Lemma 5 If and only if a path found by algorithm 3 contains sub-trajectories from two different trajectories, the two trajectories can be spliced.

Proof If there exists a path, which is found by Algorithm 3, between any two sub-trajectories from two trajectories, respectively, according to Lemma 4, the trajectories that the path passed through can be spliced with the two sub-trajectories. So, the two two sub-trajectories can be spliced. According to the definition 6, if two sub-trajectories are spliceable sub-trajectories, there exists a spliced path that can pass through all sub-trajectories of the two trajectories. □

Theorem 1 *If there exists a directed edge between two trajectories, the two trajectories can be spliced.*

Proof Suppose there is an edge between STR_i^j and STR_m^n, which the two *STR*s belong to TR_i and TR_j, respectively, and TR_i cannot be spliced with TR_m. According to Lemma 5, at least one pair of *STR*s from the two *TR*s, respectively, cannot be connected by a path that is found by $existPath$. But, a Algorithm 2 (Line 10) must have deleted all edges between TR_i and TR_j if it finds that a pair between them cannot be connected by a path. Therefore, there is not an edge between them. It contradicts the assumption that there is an edge between STR_i^j and STR_m^n.

Theorem 2 *For each $SP_i \in SP$, where SP is one of output parameters of Algorithm 2, SP_i is a set of trajectories that can be spliced with the trajectory TR_i.*

Proof At initialized phase of Algorithm 2, $SP = DT$. Suppose one SP_i has a subscript m, and its corresponding TR_m cannot be spliced with TR_i. According to Lemma 5, there is not a path between one pair $\langle STR_i^j, STR_m^n \rangle$. And, $SP_i = SP_i - m$ (Line 12 in Algorithm 2), has been executed. It contradicts with SP_i because SP_i contains m. □

Lemma 6. In *SP*-set graph, a clique is a group of spliceable trajectories, a maximal clique is a complete trajectory.

Proof A group of spliceable trajectories can be directly or indirectly spliced with each other. Therefore, there exists an edge between any two of them. So, the group of spliceable trajectories is a clique in the graph. If the clique is the maximal clique, the group of spliceable trajectories on the maximal clique cannot be contained by other groups. So, the maximal clique in the graph is a complete trajectory *CTR*. □

References

1. Bakalov P, Hadjieleftheriou M, Tsotras VJ (2005) Time relaxed spatiotemporal trajectory joins. In: Proceedings of the 13th annual ACM international workshop on geographic information systems, ACM, New York, NY, USA, pp 182–191
2. Dai J, Yang B, Guo C, Ding Z (2015) Personalized route recommendation using big trajectory data. In: 2015 IEEE 31st international conference on data engineering, pp 543–554
3. Dai J, Yang B, Guo C, Jensen CS, Hu J (2016) Path cost distribution estimation using trajectory data. Proc VLDB Endow 10(3):85–96
4. Ding Z, Yang B, Chi Y, Guo L (2016) Enabling smart transportation systems: a parallel spatio-temporal database approach. IEEE Trans Comput 65(5):1377–1391
5. Emrich T, Kriegel HP, Mamoulis N, Renz M, Züfle A (2012) Querying uncertain spatio-temporal data. In: 2012 IEEE 28th international conference on data engineering, pp 354–365
6. Eppstein D, Löffler M, Strash D (2010) Listing all maximal cliques in sparse graphs in near-optimal time. In: Algorithms and computation, no. 6506 in lecture notes in computer science, Springer Berlin Heidelberg, pp 403–414
7. Goh CH, Lu H, Ooi BC, Tan KL (1996) Indexing temporal data using existing B+-trees. Data Knowl Eng 18(2):147–165
8. Gudmundsson J, van Kreveld M (2006) Computing longest duration flocks in trajectory data. In: Proceedings of the 14th annual ACM international symposium on advances in geographic information systems, ACM, New York, NY, USA, pp 35–42
9. Gudmundsson J, van Kreveld M, Speckmann B (2004) Efficient detection of motion patterns in spatio-temporal data sets. In: Proceedings of the 12th annual ACM international workshop on geographic information systems, ACM, New York, NY, USA, pp 250–257
10. Guo C, Jensen CS, Yang B (2014) Towards total traffic awareness. SIGMOD Rec 43(3):18–23
11. Guo C, Yang B, Andersen O, Jensen CS, Torp K (2015) Ecomark 2.0: empowering eco-routing with vehicular environmental models and actual vehicle fuel consumption data. GeoInformatica 19(3):567–599
12. Guo C, Yang B, Hu J, Jensen CS (2018) Learning to route with sparse trajectory sets. In: IEEE 34th international conference on data engineering, pp 1073–1084
13. Güting RH, Valdés F, Damiani ML (2015) Symbolic trajectories. ACM Trans Spat Algorithms Syst 1(2):7:1–7:51
14. HCormen T, ELeiserson C, LRivest R, Stein C (2009) Introduction to algorithm, 3rd edn. MIT Press, Cambridge
15. Hu J, Yang B, Jensen CS, Ma Y (2017) Enabling time-dependent uncertain eco-weights for road networks. GeoInformatica 21(1):57–88
16. Hu J, Guo C, Yang B, Jensen CS (2019) Stochastic weight completion for road networks using graph convolutional networks. In: IEEE 35th international conference on data engineering, pp 1274–1285
17. Hua L, Chenjuan G, Bin Y, Christian SJ (2016) Finding frequently visited indoor pois using symbolic indoor tracking data. In: Proceedings of the 19th international conference on extending database technology, pp 449–460
18. Jensen CS, Lu H, Yang B (2009) Indexing the trajectories of moving objects in symbolic indoor space. In: International symposium on spatial and temporal databases, pp 208–227

19. Jeung H, Yiu ML, Zhou X, Jensen CS, Shen HT (2008) Discovery of convoys in trajectory databases. 1:1068–1080
20. Kieu T, Yang B, Guo C, Jensen CS (2018a) Distinguishing trajectories from different drivers using incompletely labeled trajectories. In: Proceedings of the 27th ACM international conference on information and knowledge management, pp 863–872
21. Kieu T, Yang B, Jensen CS (2018b) Outlier detection for multidimensional time series using deep neural networks. In: IEEE 19th international conference on mobile data management, pp 125–134
22. Kieu T, Yang B, Guo C, Jensen CS (2019) Outlier detection for time series with recurrent autoencoder ensembles. In: 28th international joint conference on artificial intelligence
23. Korte B, Vygen J (2012) Combinatorial optimization, algorithms and combinatorics, vol 21. Springer, Berlin
24. Lee JG, Han J, Whang KY (2007) Trajectory clustering: a partition-and-group framework. In: Proceedings of the 2007 ACM SIGMOD international conference on management of data, ACM, New York, NY, USA, pp 593–604
25. Lee JG, Han J, Li X (2015) A unifying framework of mining trajectory patterns of various temporal tightness. IEEE Trans Knowl Data Eng 27(6):1478–1490
26. Li X, Ceikute V, Jensen C, Tan KL (2013) Effective online group discovery in trajectory databases. IEEE Trans Knowl Data Eng 25(12):2752–2766
27. Li Z, Ding B, Han J, Kays R (2010) Swarm: mining relaxed temporal moving object clusters. Proc VLDB Endow 3:723–734
28. Liao L, Patterson DJ, Fox D, Kautz H (2007) Learning and inferring transportation routines. Artif Intell 171(5–6):311–331
29. Sakr MA, Güting RH (2011) Spatiotemporal pattern queries. GeoInformatica 15(3):497–540
30. Spaccapietra S, Parent C, Damiani ML, de Macedo JA, Porto F, Vangenot C (2008) A conceptual view on trajectories. Data Knowl Eng 65(1):126–146
31. Su H, Zheng K, Huang J, Wang H, Zhou X (2014) Calibrating trajectory data for spatio-temporal similarity analysis. VLDB J 24(1):93–116
32. Sun J, Tao Y, Papadias D, Kollios G (2006) Spatio-temporal join selectivity. Inf Syst 31(8):793–813
33. Tao Y, Papadias D (2001) MV3r-Tree: A spatio-temporal access method for timestamp and interval queries. In: Proceedings of the 27th international conference on very large data bases, Morgan Kaufmann Publishers Inc., San Francisco, CA, USA, pp 431–440
34. Tomita E, Tanaka A, Takahashi H (2006) The worst-case time complexity for generating all maximal cliques and computational experiments. Theor Comput Sci 363(1):28–42
35. Valdés F, Güting RH (2014) Index-supported pattern matching on symbolic trajectories. In: Proceedings of the 22Nd ACM SIGSPATIAL international conference on advances in geographic information systems, ACM, New York, NY, USA, pp 53–62
36. Vieira MR, Bakalov P, Tsotras VJ (2009) On-line discovery of flock patterns in spatio-temporal data. In: Proceedings of the 17th ACM SIGSPATIAL international conference on advances in geographic information systems, ACM, New York, NY, USA, pp 286–295
37. Wang L, Zheng Y, Xie X, Ma WY (2008) A flexible spatio-temporal indexing scheme for large-scale GPS track retrieval. In: 9th international conference on mobile data management, IEEE, pp 1–8
38. Wu H, Xue M, Cao J, Karras P, Ng WS, Koo KK (2016) Fuzzy trajectory linking. In: IEEE 32nd international conference on data engineering, IEEE, pp 859–870
39. Xie K, Deng K, Zhou X (2009) From trajectories to activities: a spatio-temporal join approach. In: Proceedings of the 2009 international workshop on location based social networks, ACM, New York, NY, USA, pp 25–32
40. Xu J, Güting RH, Zheng Y (2015) The TM-RTree: an index on generic moving objects for range queries. GeoInformatica 19(3):487–524
41. Yang B, Ma Q, Qian W, Zhou A (2009) TRUSTER: trajectory data processing on clusters. In: DASFAA, pp 768–771
42. Yang B, Guo C, Jensen CS, Kaul M, Shang S (2014) Stochastic skyline route planning under time-varying uncertainty. In: IEEE 30th international conference on data engineering, pp 136–147
43. Yang B, Guo C, Ma Y, Jensen CS (2015) Toward personalized, context-aware routing. VLDB J 24(2):297–318
44. Yang B, Dai J, Guo C, Jensen CS, Hu J (2018) PACE: a path-centric paradigm for stochastic path finding. VLDB J 27(2):153–178
45. Zheng K, Zheng Y, Yuan N, Shang S, Zhou X (2014) Online discovery of gathering patterns over trajectories. IEEE Trans Knowl Data Eng 26(8):1974–1988
46. Zheng Y (2015) Trajectory data mining: an overview. ACM Trans Intell Syst Technol 6(3):1–41

47. Zheng Y, Zhang L, Xie X, Ma WY (2009) Mining interesting locations and travel sequences from GPS trajectories. In: Proceedings of the 18th international conference on world wide web, ACM, New York, NY, USA, pp 791–800
48. Zheng Y, Xie X, Ma WY (2010) Geolife: a collaborative social networking service among user, location and trajectory. IEEE Data Eng Bull 33(2):32–39
49. Zhou P, Zhang D, Salzberg B, Cooperman G, Kollios G (2005) Close pair queries in moving object databases. In: Proceedings of the 13th annual ACM international workshop on geographic information systems, ACM, New York, NY, USA, pp 2–11

Qiang Lu received a B.S. degree from Shenyang University of Chemical Technology, Shenyang, China, in 2000 and a Ph.D. degree from China University of Petroleum-Beijing, China, 2006. From 2015 to 2016, he was a visiting scholar at the Department of Computer Science, Aalborg University, Denmark. He is currently an Associative Professor in the Department of Computer Science and Director of Computation Intelligence Center at China University of Petroleum, Beijing. He is also a faculty member in Beijing Key Lab of Petroleum Data Mining. His research interests include spatial-temporal data processing, evolutionary computing, and machine learning.

Rencai Wang received a B.S. degree from China University of Petroleum-East China, in 2014 and an M.S. degree from China University of Petroleum-Beijing, China, in 2017. He is currently working as a software engineer at IFLYTEK CO., LTD, responsible for data analysis and mining on education, and the development of the education cloud platform. His research interests include spatial–temporal data management, trajectory computing, and data mining on behaviors of the educational user.

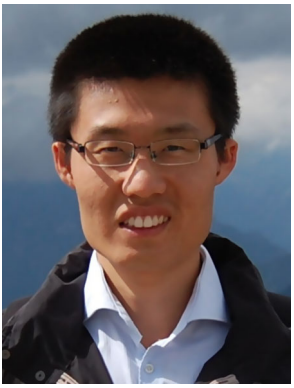

Bin Yang is a Professor in the Department of Computer Science at Aalborg University, Denmark. He was at Aarhus University, Denmark and at Max Planck Institute for Informatics, Germany. He received the Ph.D. degree in computer science from Fudan University. His research interests include machine learning and data management. He was a PC co-chair of IEEE MDM 2018. He has served on program committees and as an invited reviewer for several international conferences and journals, including ICDE, IJCAI, TKDE, the VLDB Journal, and ACM Computing Surveys.

Zhiguang Wang received a B.S. degree in physics from Inner Mongolia Normal University in 1986, an M.S. degree in computer metering from Jilin University in 1994, and a Ph.D. degree in computer science from China University of Petroleum-Beijing. He is currently a Professor in the Department of Computer Science at China University of Petroleum, Beijing, severed as Director of Research Group of Large Scale Data Processing and Visualization. He is also a faculty member in Beijing Key Lab of Petroleum Data Mining, and a council member in Beijing Education Federation. His current research interests include data management, distributed system, and spatial-temporal data mining.